Group I PAKs function downstream of Rac to promote podosome invasion during myoblast fusion in vivo

Rui Duan,[1] Peng Jin,[1] Fengbao Luo,[1] Guofeng Zhang,[2] Nathan Anderson,[1] and Elizabeth H. Chen[1]

[1]Department of Molecular Biology and Genetics, Johns Hopkins University School of Medicine, Baltimore, MD 21205
[2]Laboratory of Bioengineering and Physical Science, National Institute of Biomedical Imaging and Bioengineering, National Institutes of Health, Bethesda, MD 20892

The p21-activated kinases (PAKs) play essential roles in diverse cellular processes and are required for cell proliferation, apoptosis, polarity establishment, migration, and cell shape changes. Here, we have identified a novel function for the group I PAKs in cell–cell fusion. We show that the two *Drosophila* group I PAKs, DPak3 and DPak1, have partially redundant functions in myoblast fusion in vivo, with DPak3 playing a major role. DPak3 is enriched at the site of fusion colocalizing with the F-actin focus within a podosome-like structure (PLS), and promotes actin filament assembly during PLS invasion. Although the small GTPase Rac is involved in DPak3 activation and recruitment to the PLS, the kinase activity of DPak3 is required for effective PLS invasion. We propose a model whereby group I PAKs act downstream of Rac to organize the actin filaments within the PLS into a dense focus, which in turn promotes PLS invasion and fusion pore initiation during myoblast fusion.

Introduction

Myoblast fusion, the process in which mononucleated myoblasts fuse to form multinucleated muscle fibers, is essential for skeletal muscle development, maintenance, and satellite cell–based muscle regeneration and repair. Recent studies in the fruit fly *Drosophila* have led to the identification of evolutionarily conserved signaling pathways required for myoblast fusion (Rochlin et al., 2010; Abmayr and Pavlath, 2012). The high degree of molecular conservation between flies and vertebrates makes the relatively simple and genetically tractable *Drosophila* system particularly relevant to understanding the general mechanisms underlying myoblast fusion in vivo.

Myoblast fusion in *Drosophila* embryos commences from the recognition and adhesion between two types of muscle cells, muscle founder cells and fusion-competent myoblasts (FCMs), mediated by cell type–specific immunoglobulin (Ig) domain–containing cell adhesion molecules (Abmayr et al., 2003; Chen and Olson, 2004). The heterophilic interaction between these cell adhesion molecules, Dumbfounded (Duf)/Kirre and Roughest in muscle founder cells (Ruiz-Gómez et al., 2000; Strünkelnberg et al., 2001) and Sticks and stones (Sns) and Hibris in FCMs (Bour et al., 2000; Artero et al., 2001; Dworak et al., 2001; Galletta et al., 2004; Shelton et al., 2009), triggers intracellular signaling pathways leading to the formation of an asymmetric fusogenic synapse, which is composed of these cell adhesion molecules and morphologically distinct actin-enriched structures on either side of the adherent cell membranes (Chen, 2011; Abmayr and Pavlath, 2012). In founder cells, the fusion signal from Duf and Rst is transduced to Scar/WAVE, an actin nucleation-promoting factor (NPF) for the Arp2/3 complex (Richardson et al., 2007), resulting in the formation of a thin sheath of F-actin underlying the founder cell membrane (Sens et al., 2010). In FCMs, the fusion signal from Sns and Hbs is transduced through independent signaling pathways to two Arp2/3 NPFs, WASP (Schäfer et al., 2007) and Scar. In particular, WASP is recruited to the site of fusion (Schäfer et al., 2007; Jin et al., 2011) via its binding partner Solitary (Sltr)/WASP-interacting protein (Kim et al., 2007; Massarwa et al., 2007), whereas Scar is thought to be recruited by the small GTPase Rac (Hakeda-Suzuki et al., 2002; Gildor et al., 2009), which is

R. Duan and P. Jin contributed equally to this paper.

Correspondence to Elizabeth H. Chen: echen@jhmi.edu

Abbreviations used in this paper: AID, auto-inhibitory domain; DPak, *Drosophila* p21-activated kinase; Duf, Dumbfounded; Eve, Even skipped; FCM, fusion-competent myoblast; MHC, myosin heavy chain; NPF, nucleation-promoting factor; PAK, p21-activated kinase; PBD, p21-binding domain; PLS, podosome-like structure; Sns, Sticks and stones; Sltr, Solitary; WASP, Wiskott-Aldrich syndrome protein.

The Rockefeller University Press $30.00
J. Cell Biol. Vol. 199 No. 1 169–185
www.jcb.org/cgi/doi/10.1083/jcb.201204065

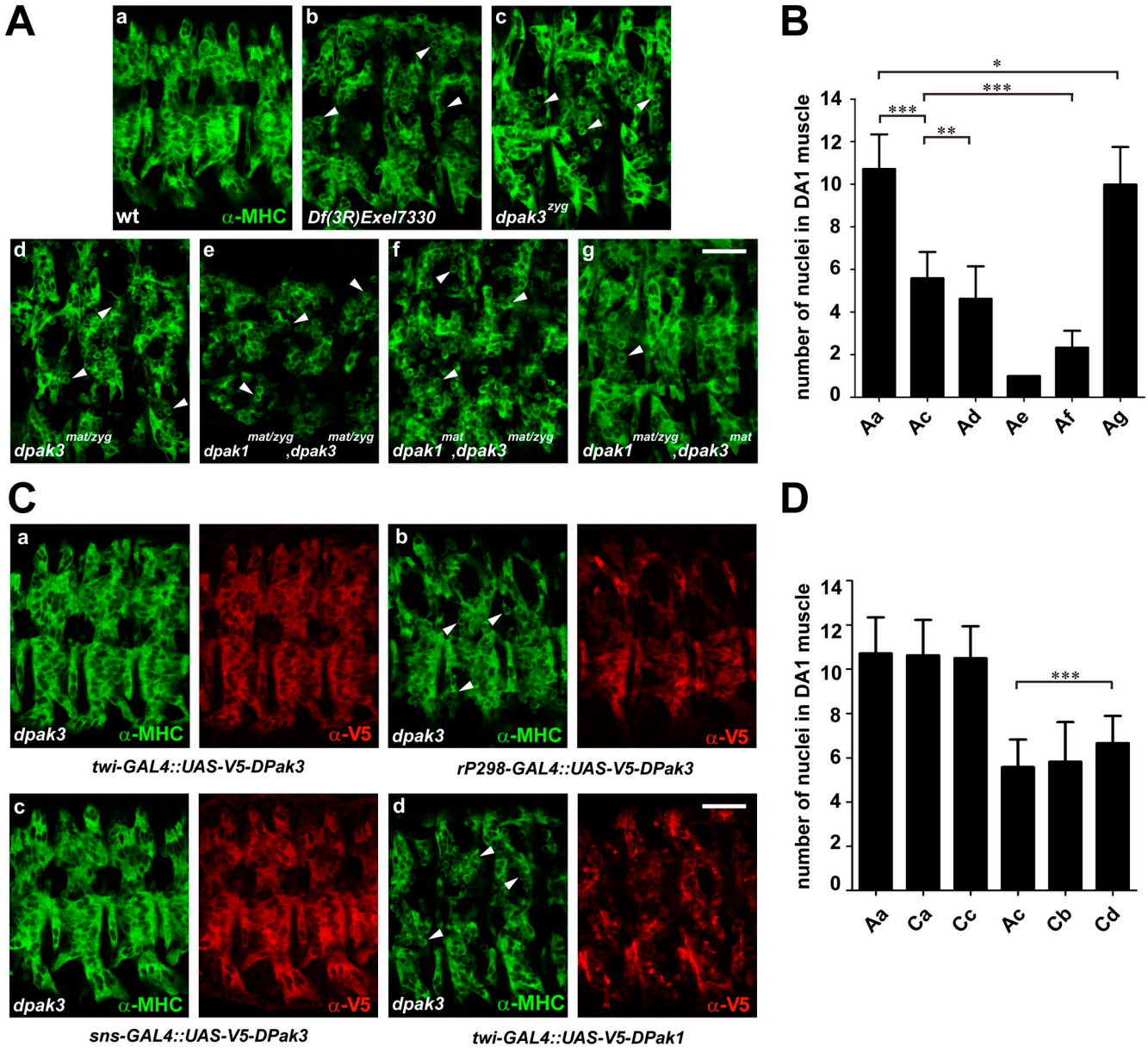

Figure 1. **DPak3 and DPak1 have partially redundant functions in myoblast fusion and are enriched at sites of fusion.** (A) Myoblast fusion is defective in *dpak3* and *dpak1* mutant embryos. Stage 15 wild-type (a, wt), *Df(3R)Exel7330* (b), $dpak3^{zyg}$ (c), $dpak3^{mat/zyg}$ (d), $dpak1^{mat/zyg}$,$dpak3^{mat/zyg}$ (e), $dpak1^{mat}$,$dpak3^{mat/zyg}$ (f), and $dpak1^{mat/zyg}$,$dpak3^{mat}$ (g) embryos labeled with a myosin heavy chain antibody (α-MHC; green). Arrowheads indicate

activated by the bipartite guanine nucleotide exchange factor (GEF), the Myoblast city–Elmo complex (Rushton et al., 1995; Erickson et al., 1997; Geisbrecht et al., 2008; Haralalka et al., 2011). Coordinated actions of WASP and Scar at the site of fusion promote actin polymerization, leading to the formation of an F-actin–enriched focus (Kesper et al., 2007; Kim et al., 2007; Richardson et al., 2007). Electron microscopy (EM) and cell type–specific GFP-actin expression experiments have unambiguously pinpointed the F-actin focus to the FCM and demonstrated that it is an integral part of an invasive podosome-like structure (PLS; Sens et al., 2010). The PLS dynamically invades the apposing founder cell/myotube with multiple finger-like protrusions to promote fusion pore formation/initiation (Sens et al., 2010; Jin et al., 2011). Consistent with the observed PLS invasion in intact embryos, FCM-associated protrusions into founder cells/myotubes have also been described in cultured *Drosophila* primary myoblasts (Haralalka et al., 2011).

The p21-activated kinases (PAKs) comprise a family of Ser/Thr kinases conserved from yeast to human. PAKs have been shown to control cell proliferation, apoptosis, gene transcription, and cytoskeletal reorganization in various cellular processes including cell adhesion, migration, invasion, and shape changes (Bokoch, 2003; Arias-Romero and Chernoff, 2008; Eswaran et al., 2008). In mammals, there are six mammalian PAKs that belong to two groups, group I (PAK1-3) and group II (PAK4-6), based on their domain architecture and regulatory mechanisms. Both group I and II PAKs contain a C-terminal catalytic domain and an N-terminal p21-binding domain (PBD) that mediates Rac–Cdc42 interaction. In addition, group I PAKs have an N-terminal auto-inhibitory domain (AID) that partially overlaps with the PBD. Biochemical and structural studies have shown that group I PAKs form auto-inhibited homodimers, in which the AID of one PAK molecule interacts in trans with the kinase domain of a second (Parrini et al., 2002). Binding of the GTP-bound, activated Rac/Cdc42 to the PBD/AID domain of a group I PAK releases the auto-inhibition, leading to an intermediary active dimer that is trans-autophosphorylated on a Thr residue in the kinase domain and several Ser residues in the N-terminal region (Benner et al., 1995; Thompson et al., 1998; Zhao et al., 1998; Gatti et al., 1999; Lei et al., 2000; Morreale et al., 2000; Chong et al., 2001; Pirruccello et al., 2006). Upon substrate binding, the PAK homodimer dissociates into monomers, which in turn phosphorylate downstream targets (Pirruccello et al., 2006).

Compared with mammals, the relatively simple *Drosophila* genome only encodes three PAKs. Two of them, DPak1 (Harden et al., 1996) and DPak3 (Mentzel and Raabe, 2005), are homologous to the mammalian group I PAKs and, in particular, PAK1 and PAK2, respectively. The third *Drosophila* PAK, Mushroom body tiny (Mbt) is a group II PAK (Schneeberger and Raabe, 2003). Although Mbt is specifically required in the nervous system, the group I DPaks have been implicated in multiple developmental and cellular processes. DPak1 has been shown to regulate dorsal closure (Conder et al., 2004), cell polarity in the ovarian follicle epithelium (Conder et al., 2007), axon and myotube guidance (Hing et al., 1999; Bahri et al., 2009), and maturation of postsynaptic terminals (Albin and Davis, 2004). The less studied DPak3 has been shown to have a redundant function with DPak1 in dorsal closure (Bahri et al., 2010) and to regulate synaptic morphology and function (Ozdowski et al., 2011).

In this study, we have identified a novel function for the *Drosophila* group I PAKs, DPak3 and DPak1, in myoblast fusion. These two PAKs are partially redundant during myoblast fusion, with DPak3 playing a more significant role than Dpak1. We show that DPak3 colocalizes with the F-actin focus within the PLS and that DPak3 recruitment to the PLS is controlled by the small GTPase Rac. Moreover, the kinase activity of DPak3 is required for PLS invasion. We propose that group I PAKs regulate actin filament assembly within the PLS to promote PLS invasion and fusion pore formation.

Results

DPak3 is required for myoblast fusion and functions specifically in FCMs

In a deficiency screen for fusion-defective mutants, we identified a third chromosome deficiency line, *Df(3R)Exel7330*. Homozygous *Df(3R)Exel7330* embryos contained many unfused myoblasts, as revealed by anti-myosin heavy chain (MHC) staining, indicating a fusion defect (Fig. 1 Ab). Of the 18 genes deleted by *Df(3R)Exel7330*, *dpak3* was identified as the sole candidate involved in myoblast fusion by dsRNA injection experiments in embryos. To confirm this, we generated a zygotic null allele of *dpak3* (*dpak3*^{zyg}) by deleting the entire *dpak3* coding sequence using a high-resolution deletion method (Parks et al., 2004). Homozygous *dpak3*^{zyg} mutant embryos showed a similar myoblast fusion defect as that of *Df(3R)Exel7330*, confirming that it is a null allele (Fig. 1 Ac). To quantify the fusion defect, we counted the number of nuclei in the dorsal anterior 1 (DA1) muscles. In wild-type embryos, 10.7 ± 1.6 (n = 42) Even skipped (Eve)–positive nuclei were present in DA1 muscles, whereas only 5.6 ± 1.2 (n = 58) Eve-positive nuclei were present in the DA1 muscles of *dpak3*^{zyg} embryos (Fig. 1 B; Table S1).

randomly selected unfused FCMs. (B) Quantification of the Eve-positive nuclei in the DA1 muscles of the different genotypes shown in A. Statistical significance was determined by unpaired student's *t* test (*, P < 0.05; **, P < 0.01; ***, P < 0.001). Error bars: standard deviations. (C) DPak3 is specifically required in FCMs. Stage 15 *dpak3*^{zyg} mutant embryos expressing indicated transgenes double labeled with α-MHC (green) and α-V5 (red). Note that V5-DPak3 expression in all mesodermal cells driven by *twi-GAL4* (a) or in FCMs driven by *sns-GAL4* (c) rescued the fusion defect. However, V5-DPak3 expression in founder cells driven by *rP298-GAL4* did not rescue the fusion defect (b). Also note that V5-DPak1 expression in the mesoderm with *twi-GAL4* resulted in a slight, but significant, rescue (d). Results of these transgenic rescue experiments are quantified in D. (E) Enrichment of DPak3 and DPak1 at sites of fusion. Stage 14 embryos triple labeled with phalloidin (green; F-actin foci), α-DPak3 or α-DPak1 (red), and α-Duf (blue; enriched at muscle cell contact sites). Note that DPak3 colocalized with the F-actin foci (arrowheads) associated with Duf accumulation in wt (a), but not *dpak3*^{zyg} mutant (b) embryos. Also note that DPak1 was not enriched at sites of fusion (arrowheads) in wt embryo (c), but was recruited to muscle cell contact sites in *dpak3*^{zyg} mutant embryo (d). Bars: (A and C) 25 µm; (E) 5 µm.

Despite the fusion defect, muscle cell fate specification, FCM migration, and muscle cell adhesion appeared normal in *dpak3*^{zyg} mutant embryos (Fig. S1) , indicating that the fusion phenotype is not a secondary consequence of defects in the early steps of myogenesis. The fusion defect in *dpak3*^{zyg} mutant embryos could be rescued by expressing a V5-tagged DPak3 (V5-DPak3) with the *twi-GAL4* driver in mesodermal cells (Fig. 1, Ca and D; Table S1), confirming that DPak3 is required for myoblast fusion.

To determine which population of muscle cells requires DPak3 function, we performed cell type–specific transgenic rescue experiments. Although V5-DPak3 expression driven by the founder cell–specific driver *rP298-GAL4* failed to rescue the fusion defect in *dpak3*^{zyg} mutant embryos (5.8 ± 1.8 nuclei in DA1, $n = 40$; Fig. 1, Cb and D; Table S1), DPak3 expression in FCMs driven by *sns-GAL4* completely rescued the fusion defect (Fig. 1, Cc and D; Table S1). Thus, DPak3 functions in the FCMs, and most likely not in founder cells, during myoblast fusion.

DPak3 colocalizes with the F-actin focus within the PLS

To understand the cellular function of DPak3 in myoblast fusion, we examined the localization of DPak3 in muscle cells. In situ hybridization revealed that *dpak3* mRNA was expressed in a broad domain in the embryo including the mesoderm (Fig. S2). To detect the DPak3 protein, we generated an anti-DPak3 antibody, which showed specificity toward DPak3 (Fig. S3). Wild-type but not *dpak3*^{zyg} mutant embryos labeled with anti-DPak3 antibody revealed punctate foci that colocalized with the F-actin foci at sites of fusion (Fig. 1, Ea and b). The localization of DPak3 to the FCM-specific F-actin foci is consistent with its specific function in FCMs, and suggests a potential role of DPak3 in regulating the PLS during myoblast fusion.

DPak1 partially compensates for DPak3 function in myoblast fusion

The partial fusion defect in *dpak3*^{zyg} mutant embryos prompted us to ask whether the *dpak3* mRNA and/or protein are maternally contributed. To test this possibility, we eliminated both maternal and zygotic functions of *dpak3* by generating germline clones of *dpak3*^{zyg}. However, *dpak3*$^{mat/zyg}$ mutant embryos only showed a slight exacerbation of the fusion defect compared with *dpak3*^{zyg}, with 4.6 ± 1.5 nuclei ($n = 37$) in the DA1 muscle (Fig. 1, Ad and B; Table S1), indicating that there is no significant maternal contribution of *dpak3* in the embryo.

We then asked whether the two group I PAKs in *Drosophila*, DPak3 and DPak1, have redundant functions during myoblast fusion. Although previous studies showed that the somatic musculature appeared normal in *dpak1* mutant embryos (Bahri et al., 2009), we hypothesized that DPak1 may compensate for DPak3 function in the absence of the latter. To test this possibility, we made double mutants of *dpak1* and *dpak3*. Although double zygotic mutant (*dpak1*^{zyg},*dpak3*^{zyg}) showed a similar myoblast fusion defect to that of *dpak3*^{zyg}, double maternal/zygotic mutant (*dpak1*$^{mat/zyg}$,*dpak3*$^{mat/zyg}$) showed a complete lack-of-fusion phenotype (1.0 ± 0.0 nucleus in DA1, $n = 11$; Fig. 1, Ae and B; Table S1). Moreover, we found that the severity of the fusion defect is dependent on the amount of residual PAK proteins in the embryo. Specifically, eliminating only the maternal function of DPak1 in *dpak3*$^{mat/zyg}$ mutant (*dpak1*^{mat},*dpak3*$^{mat/zyg}$) resulted in an intermediate fusion defect (2.3 ± 0.8 nuclei in DA1, $n = 42$; Fig. 1, Af and B; Table S1), and eliminating only the maternal function of DPak3 in *dpak1*$^{mat/zyg}$ mutant (*dpak1*$^{mat/zyg}$,*dpak3*^{mat}) resulted in a minor fusion defect (10.0 ± 1.8 nuclei in DA1, $n = 55$; Fig. 1, Ag and B; Table S1). These results demonstrate that DPak3 and DPak1 play redundant roles during myoblast fusion and that Dpak3 has a more significant function than DPak1.

To further explore the functional compensation of DPak1 for DPak3 at the cellular level, we performed antibody labeling experiments with anti-DPak1. In wild-type embryos, DPak1 enrichment was undetectable at sites of fusion marked by the F-actin foci and founder cell–specific cell adhesion protein Duf (Fig. 1 Ec). However, in *dpak3*^{zyg} mutant embryos, large aggregates of DPak1 colocalized with the F-actin foci at muscle cell contact sites (Fig. 1 Ed), suggesting that DPak1 is actively recruited to these sites to promote fusion in compensation for the loss of DPak3. In addition, overexpression of DPak1 in *dpak3*^{zyg} mutant embryos with the mesodermal *twi-GAL4* driver resulted in a slight, but significant, phenotypic rescue (6.6 ± 1.2 nuclei in DA1, $n = 59$; Fig. 1, Cd and D; Table S1). Thus, DPak1 appears to compensate for the loss of DPak3 by functioning in the F-actin foci at sites of fusion.

DPak3 genetically interacts with the Arp2/3 NPFs, WASP and Scar

Previous studies have demonstrated that formation of the F-actin focus within the PLS requires the coordinated functions of two Arp2/3 NPFs, WASP and Scar (Sens et al., 2010). The enrichment of DPak3 (and DPak1 in *dpak3*^{zyg} mutant embryos) to the F-actin foci prompted us to ask whether DPak3 genetically interacts with WASP and Scar. Due to maternal contribution, the zygotic-null mutant of *wasp* does not show a fusion defect, whereas that of *scar* exhibits a partial loss-of-fusion phenotype (5.6 ± 1.9 nuclei in DA1, $n = 36$; Kim et al., 2007; Richardson et al., 2007). However, the double mutant between *dpak3*^{zyg} and *wasp* (*dpak3,wasp*) showed a more severe fusion defect (1.9 ± 0.7 nuclei in DA1, $n = 27$; Fig. 2 A, compare a and b; Table S1) than either *dpak3*^{zyg} or *wasp* single mutant. Similarly, the double mutant between *dpak3*^{zyg} and *scar* (*scar;dpak3*) also showed an enhanced fusion defect (1.0 ± 0.0 nucleus in DA1, $n = 40$; Fig. 2 A, compare c and d; Table S1). The genetic interactions between DPak3 and the Arp2/3 NPFs strongly suggest a functional link between DPak3 and the F-actin foci at sites of fusion.

The FCM-specific F-actin foci exhibit a dispersed morphology in *dpak* mutants

To pinpoint the function of DPak3 in the F-actin foci, we analyzed the foci phenotype in *dpak3*^{zyg} mutant embryos. In wild-type embryos, myoblast fusion peaks at stage 14 (with ∼10–12 F-actin foci per hemisegment) and is largely completed by early stage 15, indicated by a significant decrease in the foci number

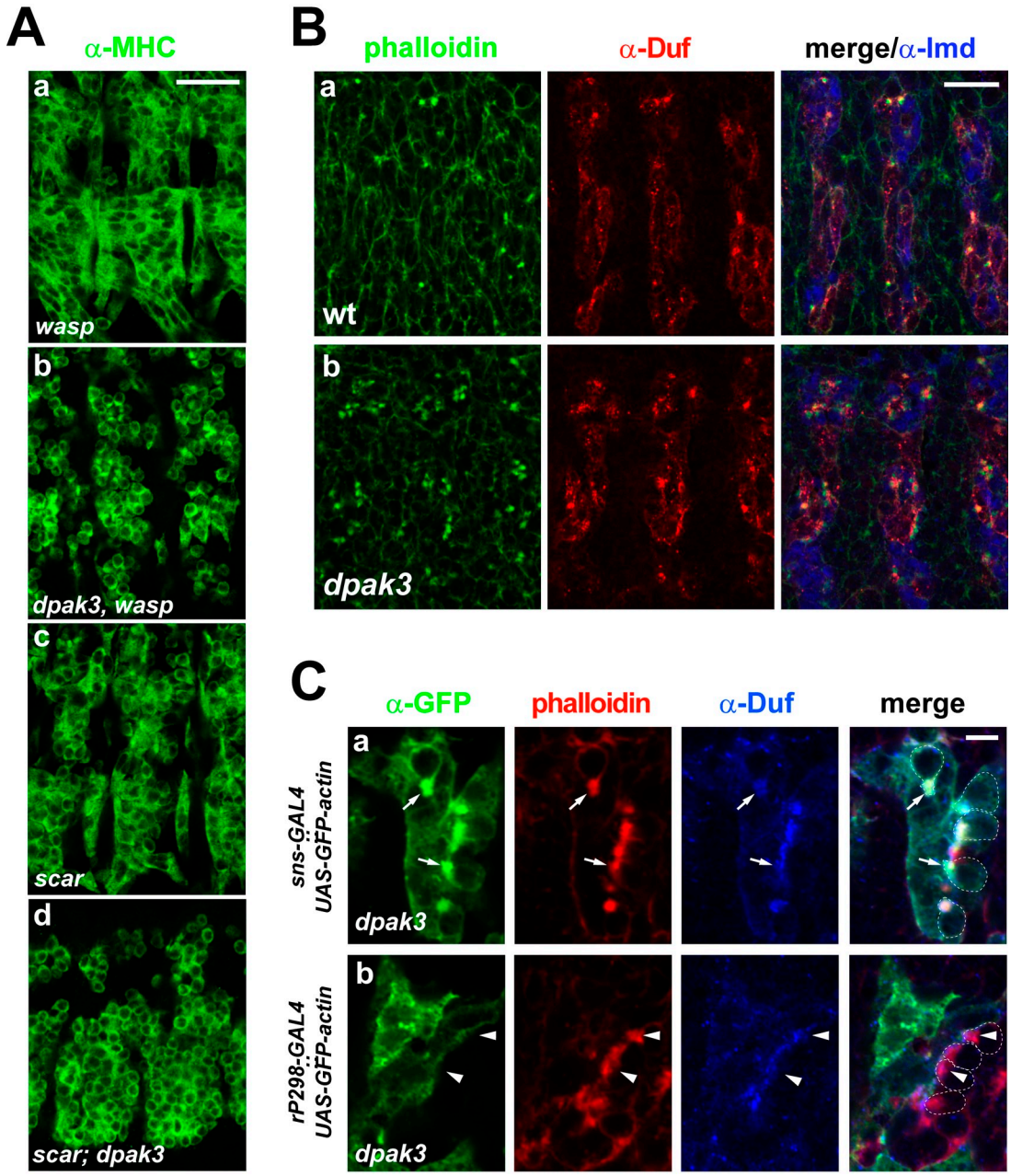

Figure 2. **The F-actin foci persist until late stages of embryogenesis and reside exclusively in FCMs in *dpak3*^{zyg} mutant embryos.** (A) DPak3 genetically interacts with the Arp2/3 NPFs WASP and Scar. Stage 15 *wasp* (a), *dpak3,wasp* (b), *scar* (c), and *scar;dpak3* (d) mutant embryos labeled with α-MHC. Note the more severe fusion defects in the double mutants compared with the respective single mutants (see Table S1 for quantification). (B) Increased F-actin foci number in *dpak3*^{zyg} mutant embryos. Late stage 14 embryos triple labeled with phalloidin (green), α-Duf (red), and α-Lame duck (Lmd, blue; FCMs; Duan et al., 2001). Three hemisegments are shown in each panel. Note that the number of F-actin foci significantly increased in *dpak3*^{zyg} mutant (b) compared with wild-type (a, wt) embryos. (C) F-actin foci are generated in FCMs of *dpak3*^{zyg} mutant embryos. Stage 14 embryos triple labeled with α-GFP (green), phalloidin (red), and α-Duf (blue). Note that GFP-actin expressed in FCMs with *sns-GAL4* colocalized with the dense F-actin foci (a, arrows), whereas GFP-actin expressed in founder cells with *rP298-GAL4* did not colocalize with the dense F-actin foci (b, arrowheads). Bars: (A and B) 25 μm; (C) 5 μm.

and the appearance of multinucleated muscle fibers. However, in the late stage 14 *dpak3*^{zyg} mutant embryos, a large number of F-actin foci (~30 foci per hemisegment) remained, indicating a failure of these foci to promote myoblast fusion (Fig. 2 B, compare a and b).

We next examined the morphology of individual F-actin foci in *dpak3*^{zyg} mutant embryos. As in wild-type embryos, the F-actin foci in *dpak3*^{zyg} mutant embryos were generated exclusively in FCMs because GFP-actin expressed in FCMs was incorporated into the F-actin foci (Fig. 2 Ca), whereas GFP-actin expressed in founder cells was not (Fig. 2 Cb). Strikingly, the majority of the FCM-specific F-actin foci in late stage 14 *dpak3*^{zyg} (Fig. 3 Ab) and *dpak3*$^{mat/zyg}$ (Fig. 3 Ac) mutant embryos displayed a more dispersed morphology than wild type (Fig. 3 Aa). In wild-type embryos, the F-actin foci exhibited a dense, solid morphology with an average fluorescence

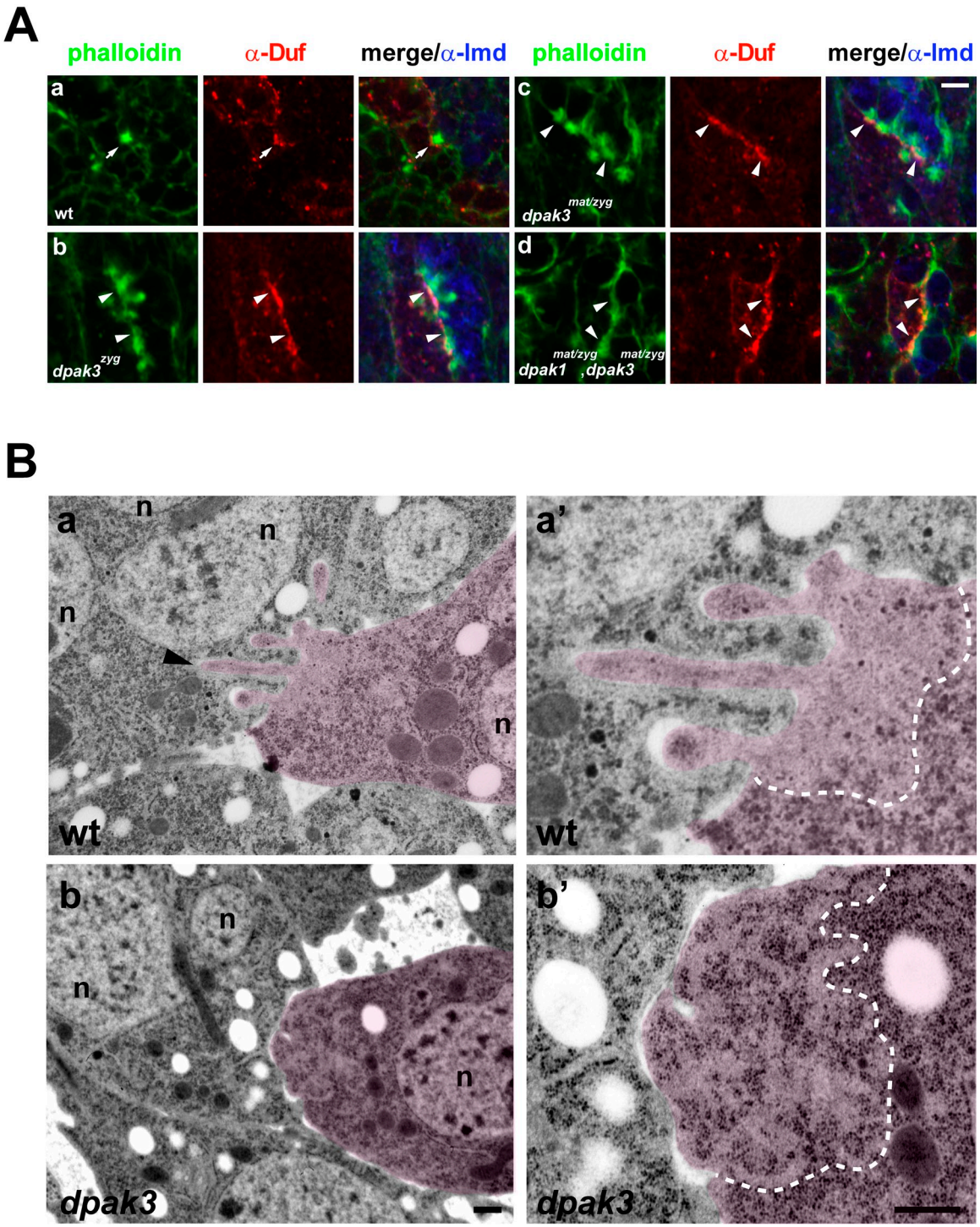

Figure 3. **Dispersed morphology of the F-actin foci and defective PLS invasion in *dpak* mutant embryos.** (A) Actin foci morphology visualized by confocal microscopy. Stage 14 embryos triple labeled with phalloidin (green), α-Duf (red), and α-Lmd (blue). Compared with the dense morphology in wild-type embryos (a, wt), the F-actin foci appeared fuzzy and dispersed in *dpak3*^{zyg} (b), *dpak3*$^{mat/zyg}$ (c), and *dpak1*$^{mat/zyg}$,*dpak3*$^{mat/zyg}$ (d) mutant embryos. Note that the dense wt actin focus caused a V-shaped inward curvature in the founder cell membrane (a, arrow). In contrast, the F-actin foci in *dpak* mutant embryos appeared dispersed and did not change the membrane curvature of the apposing founder cells (b–d, arrowheads). (B) F-actin foci visualized by EM. (a) Stage 14 wt embryo. An FCM (pseudo-colored pink) projecting multiple F-actin–enriched invasive fingers (the longest one indicated by arrowhead) into the adjacent trinucleated myotube. The protruding tip of this FCM is enlarged in (a'). Note that the F-actin–enriched area (delineated with white dashed line in a') is almost devoid of ribosomes (small black dots) and intracellular organelles, indicating the presence of a densely packed F-actin network (also see Sens et al., 2010). (b) Stage 14 *dpak3*^{zyg} mutant embryo. An FCM was in the process of invading a binucleated myotube and generated a wide, shallow dent on the myotube membrane, without projecting long, thin protrusive fingers. The tip area of the FCM is enlarged in (b'). Note that the F-actin–enriched area (delineated with white dashed line in b') contained more ribosomes than that of wt (a'), indicating the presence of loosely organized actin filaments. Also note that the cell membranes remained intact at the muscle cell contact site. n: muscle cell nuclei. Bars: (A) 5 µm; (B) 500 nm.

intensity of 167.3 ± 15.0/focus (n = 28) in a 0–255 scale measured by the LSM software. However, the F-actin foci in late stage 14 *dpak3*^{zyg} mutant embryos had an average intensity of 80.3 ± 22.9/focus (n = 43). Corresponding to the decreased intensity, the average size of the F-actin foci in *dpak3*^{zyg} mutant embryos (3.9 ± 2.1 µm^2, n = 69) was significantly larger than that of the wild-type foci (1.7 ± 0.4 µm^2, n = 21). Moreover, in *dpak1*$^{mat/zyg}$,*dpak3*$^{mat/zyg}$ double mutant embryos, the F-actin enrichment at muscle cell contact sites became even more dispersed, such that they appeared as wide "thickenings," rather than condensed foci, along the muscle cell contact zones (Fig. 3 Ad). The dispersed morphology of the F-actin foci was confirmed by EM analysis. In wild-type embryos, the area of F-actin enrichment was restricted to the protrusive tip of the FCM (Fig. 3 Ba). However, the F-actin–enriched area in the unfused FCMs of *dpak3*^{zyg} mutant embryos extended farther back into the cytoplasm (Fig. 3 Bb). In addition, unlike the F-actin–enriched areas in wild-type FCMs where the ribosomes were mostly excluded (Fig. 3 Ba′), these areas in *dpak3*^{zyg} mutant FCMs were decorated with an increased number of ribosomes (Fig. 3 Bb′), indicating the presence of loosely packed actin filaments. Consistent with the dispersed F-actin foci morphology observed in fixed embryos, live imaging of *dpak3*^{zyg} mutant embryos expressing GFP-actin with *twi-GAL4* revealed large and fuzzy mutant F-actin foci that underwent dynamic shape changes (Fig. 4 Ab; Video 2). Unlike the wild-type F-actin foci that maintained their dense morphology throughout their lifespan (Fig. 4 Aa; Video 1), each late stage 14 *dpak3*^{zyg} mutant focus appeared dispersed and disorganized, without displaying an obvious "dense core," and frequently contained clearly discernable projections and comet tail–like structures (Fig. 4 Ab). Taken together, these analyses suggest that the actin filaments within the PLS are loosely organized in *dpak3*^{zyg} mutant embryos.

The F-actin foci fail to invade founder cells or promote fusion pore formation in *dpak3* mutant embryos

The abnormal morphology of the F-actin foci in *dpak* mutants prompted us to ask whether the mutant PLSs can invade founder cells as their wild-type counterparts. In stage 14 wild-type embryos, ∼35% of the F-actin foci at a given time point appear invasive as they generate inward curvatures in the apposing founder cell/myotube membranes (Fig. 3 Aa; Sens et al., 2010). However, in late stage 14 *dpak3*^{zyg}, *dpak3*$^{mat/zyg}$, and *dpak1*$^{mat/zyg}$, *dpak3*$^{mat/zyg}$ mutant embryos, most of the F-actin foci were not associated with any inward curvature in the apposing founder cell/myotube membranes (Fig. 3 A, b–d). In the 10.5% (4/38) of the F-actin foci that appeared slightly invasive in *dpak3*^{zyg} mutant embryos, the maximum depth of invasion was 0.6 µm, compared with 1.9 µm of the wild-type foci (Sens et al., 2010). The defective PLS invasion in *dpak3*^{zyg} mutant embryos was also confirmed by EM analysis (Fig. 3, Bb and b′).

To test whether the defective PLS in *dpak3*^{zyg} mutant was capable of promoting fusion pore formation, we performed a GFP diffusion assay. As shown in Fig. 4 B, founder cell–expressed GFP (with *rP298-GAL4*) did not diffuse into the attached, mononucleated FCMs in stage 15 *dpak3*^{zyg} mutant embryos, suggesting that myoblast fusion is blocked before fusion pore formation and that DPak3 is required for fusion pore initiation. In addition, EM analysis also confirmed the absence of membrane openings abutting the dispersed F-actin foci in *dpak3*^{zyg} mutant embryos (Fig. 3, Bb and b′). These results strongly support our model that proper PLS invasion is required for fusion pore formation (Sens et al., 2010), and demonstrate a specific role for the group I PAKs in PLS invasion and fusion pore formation.

DPak3 functions downstream of Rac during myoblast fusion

To position Dpak3 in the signaling pathways controlling myoblast fusion, we first examined the localization of the known fusion proteins in *dpak3*^{zyg} mutant embryos. In FCMs, the fusion signal is transduced from the cell adhesion molecule, Sns, to the actin cytoskeleton via two independent pathways: Sns→Sltr–WASP and Sns→Rac→the Scar complex. Antibody labeling experiments showed that Sns, Sltr, and Rac remained localized with the F-actin foci at muscle cell contact sites in *dpak3*^{zyg} mutant embryos (Fig. 5 A), suggesting that DPak3 does not function upstream of these proteins to control their localization. Conversely, we examined the localization of DPak3 in several known fusion mutants. Not surprisingly, DPak3's punctate localization pattern was absent in *sns* mutant embryos (Fig. 5 Ba), consistent with the role of Sns in initiating the myoblast fusion signaling pathways in the FCM. Dpak3 remained localized to the F-actin foci in *sltr* and *kette* (encoding a component of the Scar complex; Schröter et al., 2004) mutant embryos (Fig. 5, Bb and c), suggesting that neither the Sltr–WASP nor the Scar complex is required for recruiting DPak3 to the PLS. However, the DPak3 localization to muscle cell contact sites was absent in *rac1,rac2* double mutant embryos (Fig. 5 Bd), indicating that the small GTPase Rac is involved in localizing DPak3 to the PLS. Taken together, these results suggest that DPak3 functions downstream of the Sns→Rac pathway but in parallel with the Scar complex.

Rac binding is required for DPak3's subcellular localization and function in vivo

Previous biochemical and structural studies have revealed a function for the small GTPases Cdc42/Rac in activating group I PAKs' kinase activity by binding to PAKs and releasing their trans-autoinhibition (Bokoch, 2003; Arias-Romero and Chernoff, 2008; Eswaran et al., 2008). Indeed, activated Rac (Rac^{G12V}) stimulated the auto-phosphorylation and kinase activity of DPak3 expressed in *Drosophila* S2R+ cells (Fig. 6, A–C). In addition to its ability to activate DPak3, Rac may also regulate the subcellular localization of DPak3 because DPak3 failed to localize to muscle cell contact sites in *rac1,rac2* mutant embryos (Fig. 5 Bd). Consistent with this possibility, DPak3 colocalized with Rac and the F-actin foci at sites of fusion in wild-type embryos (Fig. 5 C). To further test whether Rac binding is directly involved in regulating DPak3 localization, we took advantage of the DPak3^{H29,31L} mutant, which carried two His-to-Leu point mutations in its PBD/AID domain and failed to bind Rac in vitro (Fig. 6 D; Mentzel and Raabe, 2005). Although DPak3^{H29,31L} was defective in Rac binding, it was autophosphorylated when expressed in S2R+ cells (Fig. 6 B)

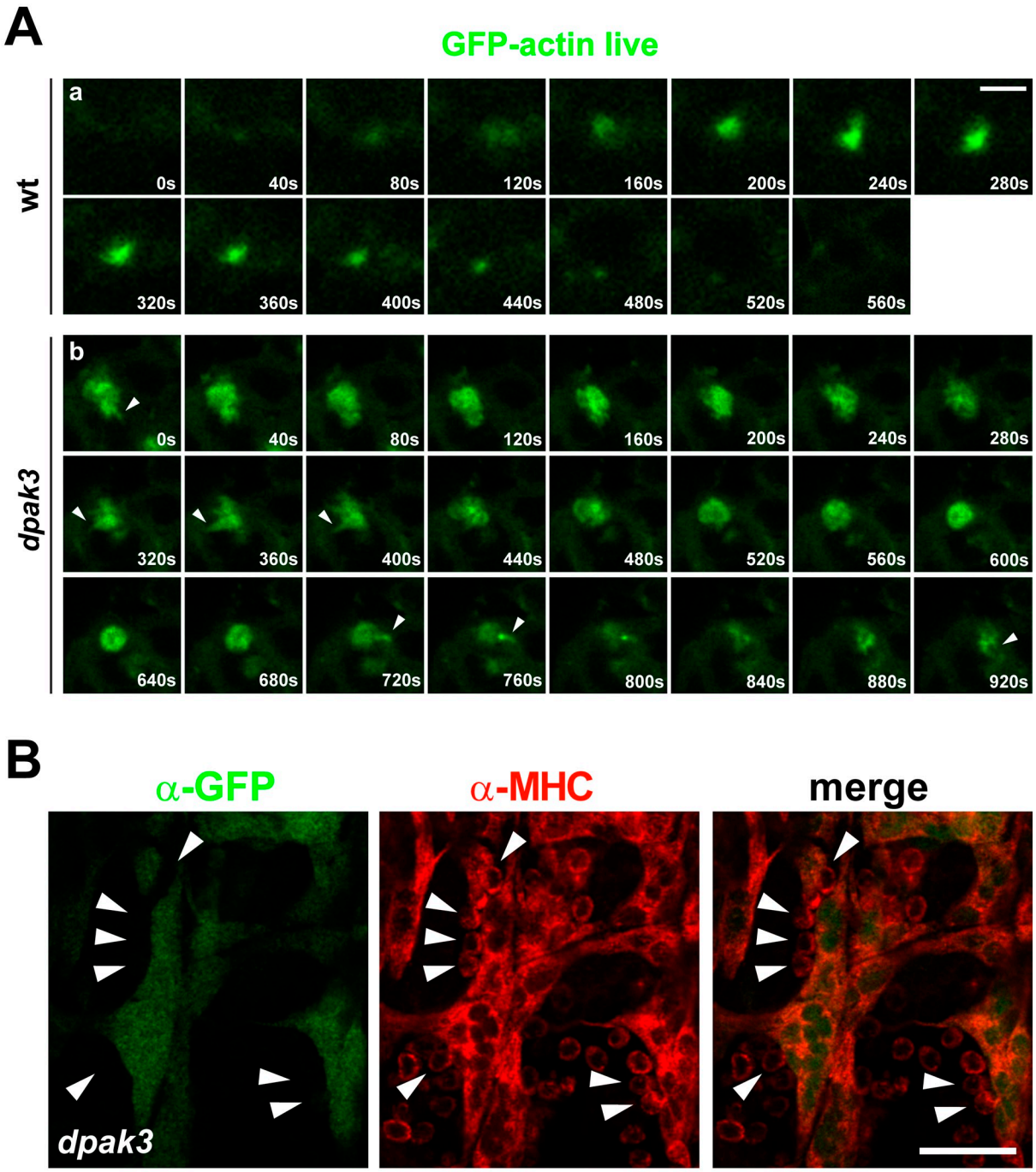

Figure 4. **Disorganized F-actin foci and failure of fusion pore formation in *dpak3* mutant embryos.** (A) Actin foci morphology visualized by live imaging. Stills from time-lapse imaging of a wild-type (a, wt) and a *dpak3*^{zyg} mutant (b) embryo expressing GFP-actin with *twi-GAL4*. Single focal planes at representative time points are shown. Note that the wt focus maintained its dense core throughout its lifespan (a). However, the *dpak3*^{zyg} mutant focus appeared to be loosely organized with clearly discernable projections and comet tail-like structures (b, arrowheads). (B) Fusion pores fail to form between founder cells/myotubes and the adherent FCMs in *dpak3*^{zyg} mutant. Cytoplasmic GFP was expressed in founder cells with *rP298-GAL4* in *dpak3*^{zyg} mutant embryos. A stage 15 embryo double labeled with α-GFP (green) and α-MHC (red). Note that the GFP signal was retained in the elongated founder cells/myotubes, without diffusing into the adherent FCMs (some indicated by arrowheads). Occasionally, *rP298-GAL4* drives leaky expression in ∼7–8% FCMs (Sens et al., 2010; Haralalka et al., 2011). Correspondingly, we observed ∼6% (22/355) GFP-positive FCMs in *rP298-GAL4::UAS-GFP-actin;dpak3*^{zyg} mutant embryos (not depicted), presumably due to the leaky expression of the *rP298-GAL4* driver. Bars: (A) 2.5 µm; (B) 20 µm.

and had constitutive kinase activity toward an exogenous substrate in vitro (Fig. 6 C; Mentzel and Raabe, 2005). We generated a transgenic line carrying V5-DPak3^{H29,31L} and tested its ability to rescue the *dpak3*^{zyg} mutant phenotype. V5-DPak3^{H29,31L}, whose expression in wild-type embryos did not cause any fusion defect, failed to rescue the fusion defect in *dpak3*^{zyg} mutant embryos (Fig. 5 D) despite its constitutive kinase activity (Fig. 6 C). Unlike V5-DPak3 that was enriched to the F-actin foci (Fig. 5 Ea), V5-DPak3^{H29,31L} was evenly distributed in the cytoplasm of muscle cells without aggregating to the F-actin foci in either wild-type or *dpak3*^{zyg}

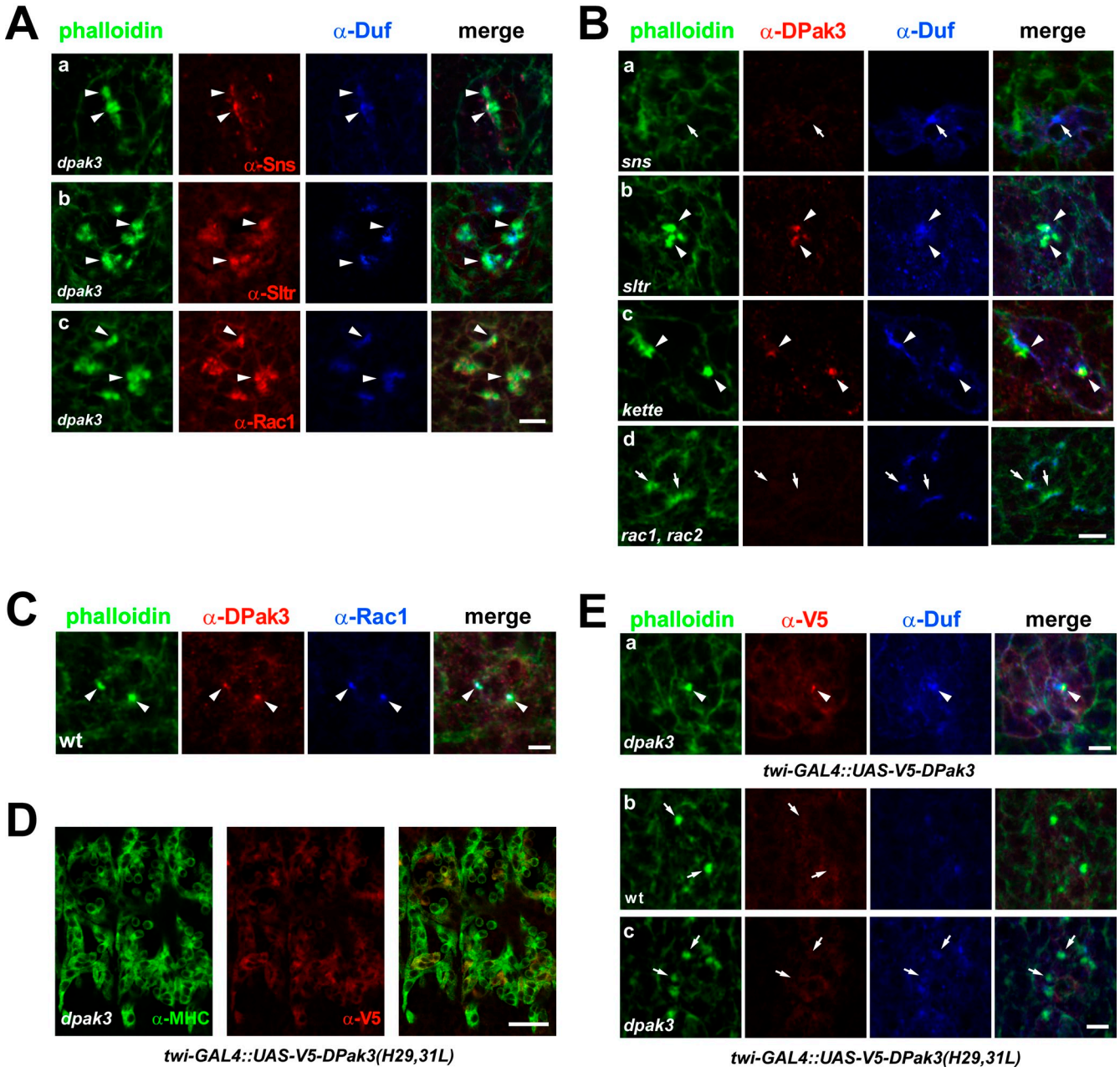

Figure 5. **Rac directly regulates DPak3 recruitment to the PLS.** (A) Sns, Sltr, and Rac remain localized with the F-actin foci in *dpak3*^{zyg} mutant embryos. Stage 14 embryos triple labeled with phalloidin (green), α-Sns (a) or α-Sltr (b) or α-Rac1 (c, red), and α-Duf (blue). (B) Localization of DPak3 in fusion mutants. Stage 14 embryos triple labeled with phalloidin (green), α-DPak3 (red), and α-Duf (blue). DPak3 was enriched in the F-actin foci (arrowheads) of *sltr* (b) and *kette* (c), but not *sns* (a) and *rac1,rac2* (d) mutant embryos. (C) Colocalization of DPak3 and Rac at sites of fusion. Stage 14 wild-type (wt) embryo triple labeled with phalloidin (green), α-DPak3 (red), and α-Rac1 (blue). (D) Transgenic rescue of *dpak3*^{zyg} mutant with V5-DPak3^{H29,31L} driven by *twi-GAL4*. Stage 15 embryo double labeled with α-MHC (green) and α-V5 (red). Note that the transgene expression failed to rescue the fusion defect. (E) DPak3$^{H29.31L}$ does not colocalize with F-actin foci at sites of fusion. Stage 14 embryos triple labeled with phalloidin (green), α-V5 (red), and α-Duf (blue). Unlike wt V5-DPak3, which was enriched at the F-actin foci (a, arrowhead), DPak3$^{H29.31L}$ was not recruited to the F-actin foci (arrows) in wt (b) or *dpak3*^{zyg} mutant (c) embryos. Bars: (A–C and E) 5 μm; (D) 20 μm.

mutant embryos (Fig. 5, Eb and c). Thus, Rac binding is directly involved in DPak3 recruitment to the PLS, and the proper subcellular localization of DPak3 is critical for its function in vivo.

The kinase activity of Dpak3 is required for PLS invasion

Although the kinase activity of Dpak3 is not sufficient for its function in myoblast fusion, we asked whether it is required. To address this question, we first examined the presence (or absence) of phosphorylated DPak3 in stage 14 embryos in which myoblast fusion is at its peak. As shown in Fig. 6 E, V5-DPak3 expressed with *twi-GAL4* in stage 14 embryos was phosphorylated, indicated by an up-shifted band on Western blot, indicating that the DPak3 kinase is activated in the mesodermal cells. Although the phosphorylation status of DPak3 within the PLS could not be assessed directly by immunohistochemistry due to the

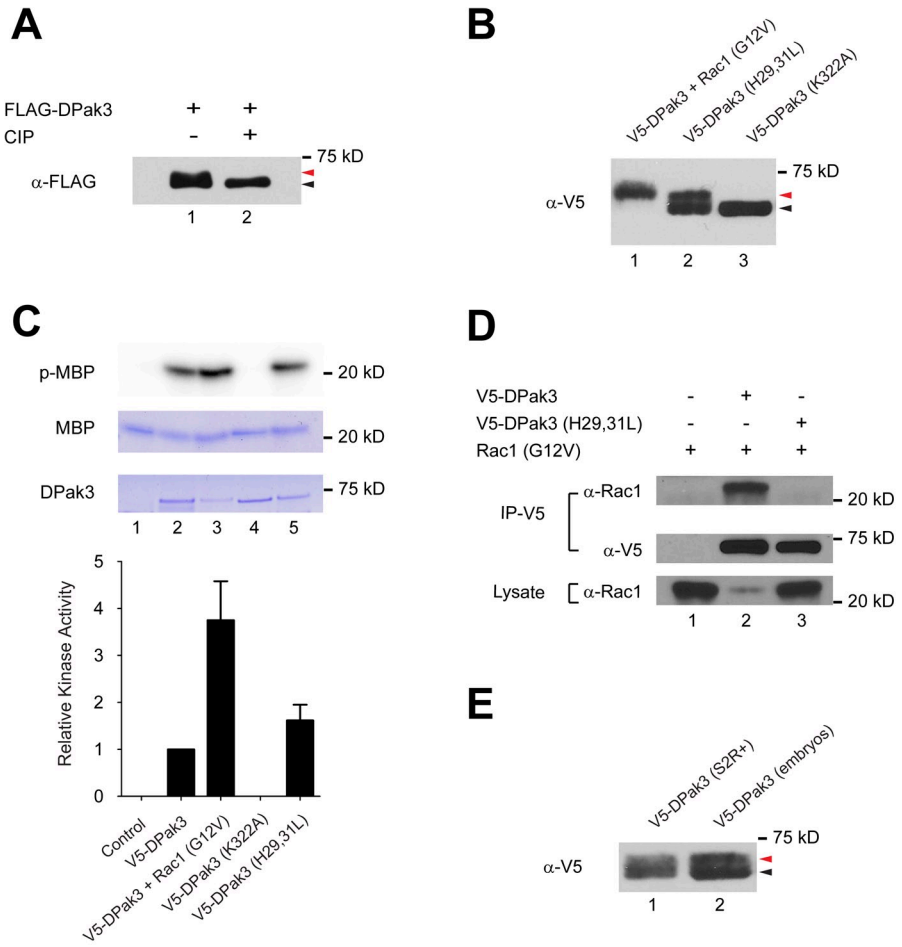

Figure 6. **Biochemical characterizations of DPak3.** (A) DPak3 is phosphorylated in S2R+ cells. FLAG-DPak3 was expressed in S2R+ cells and immunoprecipitated with α-FLAG, followed by CIP treatment. Note the disappearance of the up-shifted band of DPak3 (red arrowhead; lane 1) after CIP treatment (black arrowhead; lane 2), indicating that the up-shifted band was caused by phosphorylation. (B) Constitutively active Rac further activates DPak3 phosphorylation in S2R+ cells. DPak3 phosphorylation was further increased by coexpressing with activated Rac1 ($Rac1^{G12V}$; red arrowhead; lane 1). The Rac-binding defective mutant $DPak3^{H29,31L}$ remained partially phosphorylated (lane 2), whereas the kinase-inactive mutant was unphosphorylated (black arrowhead; lane 3). (C) In vitro kinase assays for wild-type and mutant DPak3. The kinase activities of DPak3 and its mutant forms were assessed by their ability to phosphorylate myelin basic protein (MBP) in the presence of γ-[^{32}P]ATP. Expression of MBP and different DPak3 proteins was detected by Coomassie brilliant blue staining. The kinase activities were normalized against protein expression levels and compared with that of V5-DPak3. Results from three independent experiments were quantified. Note the great increase in the DPak3 kinase activity when it was coexpressed with activated Rac1 (lane 3), the complete loss of kinase activity resulting from the K322A mutation (lane 4), and the constitutive kinase activity of $DPak3^{H29,31L}$ (lane 5). Error bars: standard deviations. (D) DPak3, but not $DPak3^{H29,31L}$, interacts with activated Rac1 ($Rac1^{G12V}$) expressed in S2R+ cells (compare lanes 2 and 3). (E) DPak3 is phosphorylated in stage 14 *Drosophila* embryos. Extracts prepared from stage 14 embryos expressing V5-DPak3 in the mesoderm with *twi-GAL4* were subjected to SDS-PAGE (lane 2), together with an extract of S2R+ cells expressing V5-DPak3 as a control (lane 1). Note the similarly up-shifted bands in both lanes (red arrowhead), indicating phosphorylation of V5-DPak3 in vivo. Percentage of the polyacrylamide gels: 6% in A, B, and E; 15% in C; and 12% in D.

unavailability of a phospho-specific antibody against DPak3, we took advantage of a kinase-inactive mutant of DPak3 to examine the requirement of its kinase activity during myoblast fusion. Previous biochemical experiments revealed that a Lys-to-Ala substitution in the kinase domain of DPak3 ($DPak3^{K322A}$) abolishes ATP binding and renders the kinase inactive without affecting Rac binding (Mentzel and Raabe, 2005). Consistent with this, $DPak3^{K322A}$ was unphosphorylated when expressed in S2R+ cells (Fig. 6 B) and had no kinase activity toward an exogenous substrate (Fig. 6 C). We performed a transgenic rescue experiment by expressing $DPak3^{K322A}$ in the mesoderm of $dpak3^{zyg}$ mutant embryos. Overexpressing an N-terminally tagged DPak3 ^{K322A} ($V5\text{-}DPak3^{K322A}$) at 25°C, which did not cause any muscle phenotype in wild-type embryos, failed to rescue the fusion defect in $dpak3^{zyg}$ mutant embryos (5.4 ± 1.3 nuclei in DA1, $n = 46$; Fig. 7, Ab and B; Table S1). Strikingly, $V5\text{-}DPak3^{K322A}$ properly localized to the PLS, but failed to rescue PLS invasion into founder cells/myotubes (Fig. 7 Ca). Only 9.7% (6/62) of the F-actin foci appeared slightly invasive in these embryos, and the maximum depth of invasion was 0.5 µm. Taken together, these results demonstrate that the kinase activity of DPak3 is required for promoting PLS invasion during myoblast fusion.

Previous studies have shown that the kinase-inactive form of mammalian PAK1 behaves in a dominant-negative manner to compete with endogenous PAK1 for substrate binding by forming nonproductive kinase–substrate complexes (Morita et al., 2007; Tang et al., 1997). Interestingly, overexpressing the N-terminally tagged $V5\text{-}DPak3^{K322A}$ at 30°C resulted in mutant kinase accumulation in the PLS (Fig. 7 Cb) and an enhancement of the fusion defect (3.6 ± 1.3 nuclei in DA1, $n = 60$; Fig. 7, Ac and B; Table S1). Moreover, overexpressing a C-terminally tagged DPak3 ^{K322A} ($DPak3^{K322A}$-V5) at 25°C resulted in a near complete block of myoblast fusion (1.4 ± 0.7 nuclei in DA1, $n = 34$; Fig. 7, Ad and B; Table S1), accompanied by an even higher accumulation of the mutant kinase in the PLS (Fig. 7 Cc). In these embryos, the F-actin foci appeared more dispersed than those in $dpak3^{zyg}$ mutant embryos, with an average fluorescence intensity of 66.7 ± 22.4/focus ($n = 60$; Fig. 7 Cc). Correspondingly, less

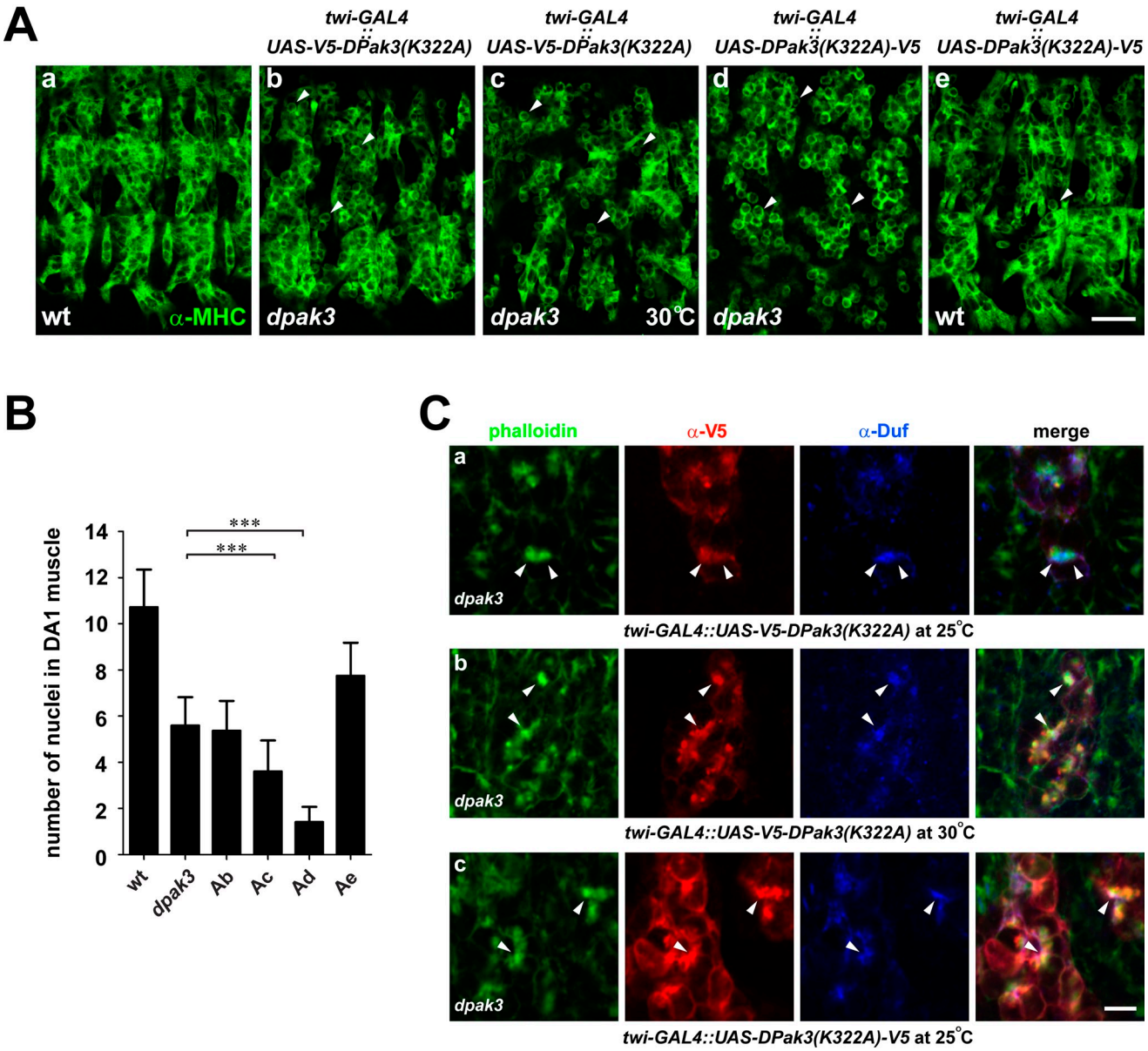

Figure 7. **The kinase activity of DPak3 is required for PLS invasion.** (A) Stage 15 wild-type (a and e, wt) or *dpak3*^{zyg} mutant (b–d) embryos carrying indicated transgenes were labeled with α-MHC. V5-DPak3^{K322A} expression at 25°C failed to rescue the fusion defect in *dpak3*^{zyg} mutant embryos (b) and at 30°C resulted in a more severe fusion defect (c). DPak3^{K322A}-V5 expression at 25°C enhanced the fusion defect in *dpak3*^{zyg} mutant embryos (d, compare with b), and resulted in a minor fusion defect in wild-type embryos (e, compare with a). Arrowheads indicate randomly selected unfused FCMs. (B) Quantification of the fusion defects in the genotypes shown in A. Statistical significance was determined by unpaired student's *t* test (***, $P < 0.001$). Error bars: standard deviations. (C) Localization of overexpressed DPak3^{K322A} to muscle cell contact sites. Stage 14 embryos triple labeled with phalloidin (green), α-V5 (red), and α-Duf (blue). V5-DPak3^{K322A} localized to the muscle cell contact sites (arrowheads) indicated by F-actin foci and Duf enrichment at 25°C (a), and accumulated at a higher level to these sites at 30°C (b). The C-terminally tagged DPak3^{K322A}-V5 showed an even higher accumulation to these sites at 25°C (c) than V5-DPak3^{K322A} at 30°C (b). All images were acquired by the same confocal settings. Note that the F-actin foci did not cause V-shaped curvatures in the founder cell membranes marked by Duf enrichment. Bars: (A) 25 µm; (C) 5 µm.

than 7% (2/29) of F-actin foci appeared slightly invasive, and the maximum depth of invasion was 0.4 µm. Furthermore, DPak3^{K322A}-V5 expression in the mesoderm of wild-type embryos at 25°C resulted in a minor fusion defect (7.4 ± 1.4 nuclei in DA1, $n = 43$; Fig. 7, Ae and B; Table S1). Thus, the kinase-inactive form of DPak3 functions in a dominant-negative manner and, when expressed at a high level, interferes with the function of DPak3 (in wild-type embryos) and DPak1 (in *dpak3*^{zyg} mutant embryos) during myoblast fusion.

Discussion

Group I PAKs have partially redundant functions in myoblast fusion

The PAK family of Ser/Thr kinases have been implicated in many biological processes, including cell migration, invasion, proliferation, and survival, as well as regulation of neuronal outgrowth, hormone signaling, and gene transcription (Bokoch, 2003; Arias-Romero and Chernoff, 2008; Eswaran et al., 2008).

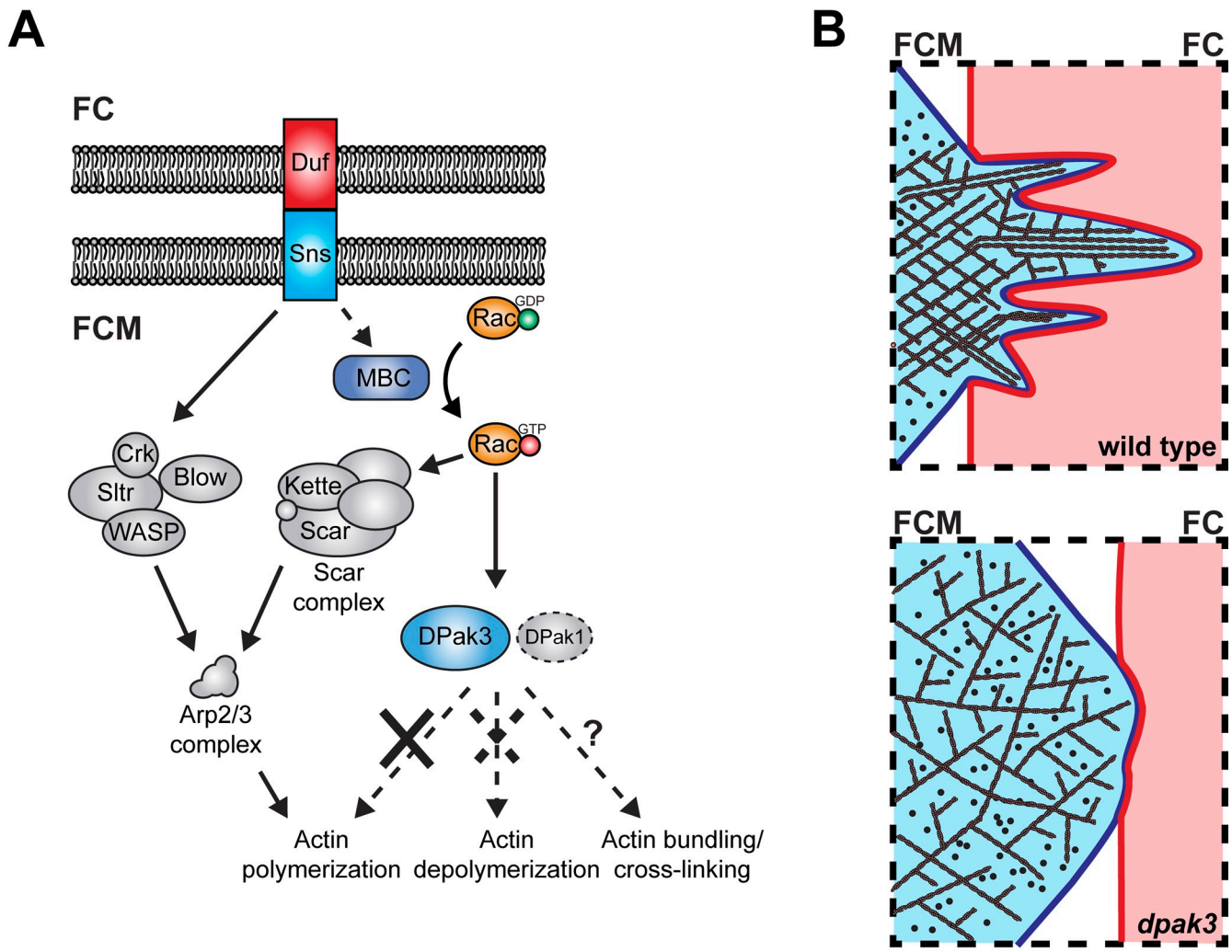

Figure 8. **Models describing the proposed function of group I PAKs in myoblast fusion.** (A) Group I PAKs act directly downstream of the small GTPase Rac, and in parallel with the Scar and WASP complexes, to promote myoblast fusion. DPak3 and DPak1 are partially redundant, with DPak3 playing a more significant role, in the fusion process. PAKs do not appear to affect actin polymerization or depolymerization, but may regulate actin bundling/cross-linking proteins during myoblast fusion. (B) Group I PAKs regulate podosome invasion during myoblast fusion. In wild-type embryos, PAKs organize the Arp2/3-nucleated, branched actin filaments within the PLS into a densely packed structure (devoid of ribosomes indicated by black dots), which, in turn, efficiently invades the apposing founder cell (FC)/myotube with multiple finger-like protrusions and ultimately leads to fusion pore formation. PAKs may do so by activating actin bundling/cross-linking proteins (A), allowing the formation of highly stiff actin bundles that exert large protrusive forces against the cell membrane. In *dpak* mutant embryos, the actin filaments are disorganized and dispersed (the actin-enriched area decorated with ribosomes), resulting in a failure in PLS invasion and fusion pore formation.

However, a role for PAKs in muscle development and cell–cell fusion has not been previously uncovered. In this study, we reveal an essential function for *Drosophila* group I PAKs during myoblast fusion in vivo (Fig. 8 A). Specifically, we show that the two group I PAKs in *Drosophila*, DPak3 (a close homologue of mammalian PAK2) and DPak1 (a close homologue of mammalian PAK1), have partially redundant functions in myoblast fusion, based on the following lines of evidence. First, double and single mutants of *dpak3* and *dpak1* exhibited a range of fusion defects ($dpak1^{mat/zyg}$,$dpak3^{mat/zyg} > dpak1^{mat}$,$dpak3^{mat/zyg} > dpak3^{mat/zyg} \geq dpak3^{zyg} = dpak1^{zyg}$,$dpak3^{zyg} > dpak1^{mat/zyg}$,$dpak3^{mat} \geq dpak1^{mat/zyg} = dpak1^{zyg}$), dependent on the residual endogenous protein level. Clearly, DPak3 plays a more significant role than DPak1, and the minor role of DPak1 can only be revealed in the context of the *dpak1,dpak3* double mutant. Second, DPak3 is enriched in the F-actin foci in wild-type embryos. On the other hand, DPak1 only accumulates in the F-actin foci in the absence of DPak3, consistent with its compensatory function in the fusion process. Third, overexpression of DPak1 in the $dpak3^{zyg}$ mutant leads to a slight but reproducible rescue of fusion. Finally, overexpression of a kinase-inactive form of DPak3 ($DPak3^{K322A}$) in $dpak3^{zyg}$ mutant embryos significantly enhances the fusion defect, presumably by forming nonproductive $DPak3^{K322A}$–substrate complexes that exclude DPak1.

What accounts for the differential effects of DPak3 and DPak1 in myoblast fusion? One possibility is that DPak3 is recruited to the PLS at a higher level than DPak1 in wild-type embryos. However, the different recruitment levels cannot solely account for the differential effects of these two proteins because DPak1 overexpression in $dpak3^{zyg}$ mutant embryos does not

completely rescue the fusion defect. A second possibility is that DPak3 and DPak1 may have different interacting partner(s) in the PLS, and thus may respond differently to upstream Rac signaling and/or transduce different downstream signals. In this regard, it has been reported that human PAK2, but not PAK1, can interact with MYO18A, which is involved in actin filament organization and cell migration (Hsu et al., 2010). A third possibility is that these two kinases may have intrinsic differences in substrate binding affinity and/or kinase activity. For example, DPak3 may preferentially bind and activate specific substrates in wild-type embryos and DPak1 could only access and/or inefficiently activate these substrates in the absence of DPak3. In support of this hypothesis, expressing the kinase-inactive from of DPak3 ($DPak3^{K322A}$) in the *dpak3*^{zyg} mutant abolishes the functional compensation by DPak1, suggesting that $DPak3^{K322A}$ may efficiently compete with DPak1 for substrate binding by forming high-affinity $DPak3^{K322A}$–substrate complexes. Obviously, identification of the preferred substrates of these group I PAKs in vivo will be required to further test this hypothesis.

The subcellular localization of DPak3 is controlled directly by Rac binding

Previous studies have shown that the activity of group I PAKs is regulated by the small GTPases Rac/Cdc42. The subcellular localization of group I PAKs, on the other hand, is thought to be controlled by SH2-SH3 domain-containing small adaptor proteins Nck and Grb (Bokoch, 2003; Arias-Romero and Chernoff, 2008; Eswaran et al., 2008). Although the expression of a dominant-negative form of Rac resulted in a loss of DPak1 localization at the leading edge during dorsal closure in *Drosophila* embryos (Harden et al., 1996), it was unclear if Rac directly regulates DPak1 recruitment to the leading edge. Here, we provide evidence that the localization of DPak3 to a specific subcellular structure, the F-actin focus within the PLS, is directly controlled by Rac. First, Rac colocalizes with DPak3 within the F-actin foci during myoblast fusion. Second, DPak3 is no longer localized to the F-actin foci in *rac1,rac2* double mutant embryos. Third, DPak3 carrying mutations in the Rac-binding domain ($DPak3^{H29,31L}$) fails to localize to the F-actin foci or rescue the *dpak3*^{zyg} mutant phenotype, despite its constitutive kinase activity. We note that although the subcellular localization of group II PAKs has been shown to be controlled by Cdc42 in cultured mammalian cells (Abo et al., 1998) and in *Drosophila* photoreceptor cells (Schneeberger and Raabe, 2003), our study reveals, for the first time, such a localization mechanism for a group I PAK. Moreover, our study has positioned group I PAKs in a new signaling branch downstream of the Rac GTPase during myoblast fusion, in addition to the previously known branch involving the Scar complex (Fig. 8 A).

Group I PAKs regulate podosome invasion

Mammalian group I PAKs have been implicated in regulating podosome formation, size, and number in cultured cells (Webb et al., 2005; Gringel et al., 2006; Morita et al., 2007). However, the function of PAKs in individual podosomes, especially in intact organisms, remained completely unknown. Our current study demonstrates that group I PAKs are required for regulating the invasive behavior of individual podosomes in an intact organism. We show that DPak3 is required specifically in the FCMs and colocalizes with the F-actin foci within the PLS. We also show that in *dpak3*^{zyg}, *dpak3*$^{mat/zyg}$, and *dpak1*$^{zyg/mat}$,*dpak3*$^{mat/zyg}$ mutants, the F-actin foci persisting to late developmental stages appear dispersed and fail to invade into the apposing founder cells/myotubes. As a result, fusion pores fail to form between these defective FCMs and their apposing founder cells/myotubes. Thus, our current study not only strongly supports our model that PLS invasion is required for fusion pore formation, but also reveals, for the first time, that group I PAKs are important regulators of podosome invasion in vivo.

How do group I PAKs regulate PLS invasion? The dispersed morphology of the F-actin foci in *dpak3*^{zyg} and *dpak1*$^{zyg/mat}$, *dpak3*$^{mat/zyg}$ mutants suggests that group I PAKs may be involved in organizing branched actin filaments into a dense focal structure within the PLS. Because the kinase activity of DPak3 is required for its function during myoblast fusion, DPak3 may regulate actin cytoskeletal remodeling by phosphorylating downstream substrates associated with the actin cytoskeleton, such as regulators of actin polymerization, depolymerization, and/or actin filament bundling/cross-linking (Fig. 8 A). Our genetic and immunohistochemical analyses suggest that DPak3 is unlikely to promote actin polymerization via the Arp2/3 NPFs WASP and Scar, because DPak3 functions in parallel with the WASP and Scar complexes and the amount of F-actin in each PLS is not markedly reduced in *dpak3*^{zyg} mutant embryos. In addition, DPak3 is unlikely to suppress actin depolymerization via PAK's well-characterized substrate, LIM kinase (LIMK), because loss-of-function mutants of LIMK and its substrate, the actin depolymerization factor cofilin, did not have a myoblast fusion defect, and DPak3 did not show genetic interactions with LIMK or cofilin during myoblast fusion (unpublished data). Therefore, it is conceivable that the group I PAKs may regulate actin bundling and/or cross-linking proteins, which, in turn, organize the assembly of branched actin filaments into tightly packed bundles to promote PLS invasion (Fig. 8 B). In this regard, it has been shown that a tight intermolecular packing of the actin filaments mediated by actin cross-linkers leads to the formation of highly stiff actin bundles that exert large protrusive forces against the cell membrane (Claessens et al., 2006). Future experiments are required to identify the bona fide downstream substrate(s) of DPak3 in regulating PLS invasion during myoblast fusion.

Interestingly, mammalian group I PAKs have been associated with cellular invasion of other cell types, such as cancer cells during metastasis (Vadlamudi and Kumar, 2003; Molli et al., 2009; Whale et al., 2011). Elevated expression and hyperactivity of PAK1 and PAK2 are seen in several types of tumors (Molli et al., 2009). Overexpression of constitutively active PAK1 promotes cancer cell migration and invasion, whereas inhibiting PAK1 suppresses these phenotypes (Adam et al., 2000; Vadlamudi et al., 2000; Stofega et al., 2004; Arias-Romero et al., 2010). It is well known that cancer cell invasion is mediated by invadopodia, which are podosome-like structures with larger F-actin–enriched cores and less dynamic actin polymerization (Weaver, 2006). A role of PAK1 and PAK2 in invadopodia

formation in an invasive metastatic human melanoma cell line has been revealed (Ayala et al., 2008). Thus, further studies of PAK function in podosome invasion in *Drosophila* myoblast fusion will not only provide additional insights into muscle differentiation, but also cancer cell invasion during tumorigenesis.

Materials and methods

Fly genetics

Fly stocks were obtained from the Bloomington Stock Center except for the following: w^{1118},$sltr^{S1946}$/CyO,*actin-lacZ* (Kim et al., 2007); $kette^{J4\text{-}48}$/*TM6B* (Hummel et al., 2000); $scar^{\Delta 37}$/CyO (Zallen et al., 2002); FRT^{82B},$wasp^{3}$,*e*/*TM6B* (Ben-Yaacov et al., 2001); $sns^{40\text{-}49}$/CyO (Paululat et al., 1999); *sns-GAL4* (Kocherlakota et al., 2008); *rP298-GAL4* (Menon and Chia, 2001); and *P{XP}pak3*^{d02472} and *PBac{RB}pak3*^{e00329} (Exelixis Collection, Harvard Medical School, Boston, MA).

A null allele of *dpak3*, *dpak3*^{zyg}, was generated by deleting the entire *dpak3* coding sequence between *P{XP}pak3*^{d02472} and *PBac{RB}pak3*^{e00329}.

Transgenic lines containing (1) *UAS-V5-DPak3*; (2) *UAS-V5-DPak3*^{H29,31L}; (3) *UAS-V5-DPak3*^{K322A}; (4) *UAS-DPak3*^{K322A}*-V5*; and (5) *UAS-V5-DPak1* were generated by standard P-element–mediated transformation.

Transgenic rescue crosses were performed by crossing female *dpak3*^{zyg} mutant flies carrying a transgene with males of (1) *rP298-GAL4/Y;dpak3*^{zyg}*/TM3,ftz*-lacZ; (2) *sns-GAL4;dpak3*^{zyg}*/TM3,ftz-lacZ*; or (3) *twi-GAL4;dpak3*^{zyg}*/TM3,ftz-lacZ*. Mutant embryos were identified by the lack of anti–β-gal staining. Transgene expression was confirmed by anti-V5 staining. Two independent transgenic lines were tested for each rescue experiment.

Expressing GFP-actin in *dpak3*^{zyg} mutant embryos: *dpak3*^{zyg}*,UAS-Act5C.GFP3/TM3,ftz-lacZ* females were crossed with males of (1) *rP298-GAL4/Y;dpak3*^{zyg}*/TM3,ftz*-lacZ; (2) *sns-GAL4;dpak3*^{zyg}*/TM3,ftz-lacZ*; or (3) *twi-GAL4;dpak3*^{zyg}*/TM3,ftz-lacZ*. In all crosses, mutant embryos were identified by the lack of β-gal expression in fixed samples or by the fusion-defective phenotype in live samples.

GFP diffusion assay: *rP298-GAL4/Y;dpak3*^{zyg}*/TM3,ftz*-lacZ males were crossed with *dpak3*^{zyg}*,cytoGFP/TM3,ftz-lacZ* females. Mutant embryos were identified by anti-MHC staining.

Molecular biology

Full-length *dpak3* and *dpak1* were amplified by PCR with an N-terminal or a C-terminal V5 tag from cDNA clones LD10326 and LD20767 from the Drosophila Genomics Resource Center (DGRC, Bloomington, IN). These PCR fragments were then subcloned into the pAc vector for expression in S2R+ cells or the pUAST vector for generating transgenic lines.

dpak3^{K322A},*dpak3*^{H29,31L} and *rac1*^{G12V} were generated using a standard site-directed mutagenesis protocol (Agilent Technologies) to introduce mutations into *dpak3* and *rac1*, respectively, followed by subcloning of the mutant cDNAs into the pAc-V5 or pUAST vectors. All constructs were verified by sequencing analysis.

Immunohistochemistry

Embryos were fixed and stained as described previously (Sens et al., 2010). In brief, embryos were fixed in 4% formaldehyde/heptane for 20 min, then devitellinized and stored in methanol. Primary and secondary antibodies were added and incubated overnight at 4°C. For phalloidin staining, embryos were fixed in 4% formaldehyde/heptane for 20 min, then hand-devitellinized in PBST. FITC-conjugated phalloidin (Invitrogen) was diluted to 20 µM in methanol and used at 1:250 along with primary and secondary antibodies. The following primary antibodies were used: rabbit anti-MHC (1:1,000; Kiehart and Feghali, 1986); rabbit anti-GFP (1:1,000; Molecular Probes); mouse anti–β-gal (1:1,000; Promega); mouse anti-Eve (1:30; Developmental Studies Hybridoma Bank, Iowa City, IA); mouse anti-Rac1 (1:200; BD); guinea pig anti-Duf (1:250; Sens et al., 2010); rabbit anti-DMef2 (1:100, Nguyen et al., 1994) and rabbit anti-DPak1 (1:2,000; Harden et al., 1996). The rat anti-DPak3 antiserum was generated against an N-terminal peptide (MSFTKWFKKKGGDGGSISEI; Biosynthesis) and used at 1:100. Secondary antibodies used at 1:300 were: FITC-, Cy3-, and Cy5-conjugated antibodies made in goat (Jackson ImmunoResearch Laboratories, Inc.).

In situ hybridization

A DIG-labeled probe was prepared using a 600-bp fragment of the coding sequence of *dpak1* (or *dpak3*) with the RNA DIG labeling kit (Roche). Fixation, post-fixation, hybridization, and development of wild-type embryos were performed according to a detailed online protocol (http://www.biology.ucsd.edu/~davek/).

Biochemistry

For coimmunoprecipitation assays, expression constructs were transfected in S2R+ cells. Cells were harvested, washed with PBS, and incubated in NP-40–Triton buffer (10 mM Tris, pH 7.4, 150 mM NaCl, 1 mM EDTA, 1% Triton X-100, and 0.5% NP-40) containing 1 mM PMSF and protease inhibitor cocktail (Roche) for 30 min at 4°C with agitation. After centrifugation, the cleared supernatants were incubated with the indicated antibodies at 4°C for 1 h, followed by immunoprecipitation with protein G beads for 2 h. After washing, immunoprecipitated proteins were subjected to SDS-PAGE and Western blot. Antibodies used for immunoprecipitation: mouse anti-V5 (1:500; Invitrogen) and mouse anti-FLAG (1:500; Sigma-Aldrich); for Western blot: mouse anti-V5-HRP (1:5,000; Invitrogen) and mouse anti-FLAG-HRP (1:5,000; Sigma-Aldrich).

For phosphatase (CIP) treatment, FLAG-DPak3 was expressed in S2R+ cells and harvested as described above. The FLAG-DPak3 protein was immunoprecipitated with anti-FLAG M2 affinity gel (A2220; Sigma-Aldrich), and the immunoprecipitated protein was then incubated in phosphatase buffer (B7003; New England Biolabs, Inc.) with or without 100 U/ml CIP (M0290; New England Biolabs, Inc.) at 37°C for 30 min. Subsequently, the samples were subjected to Western blot.

For in vitro kinase assays, V5-tagged DPak3 and its mutant forms were expressed in S2R+ cells and immunoprecipitated with anti-V5 antibody as described above. The immunoprecipitated proteins were washed three times in the NP-40–Triton buffer, once in 0.5 M NaCl, and two times in ice-cold kinase buffer (20 mM Hepes, pH 7.6, 2 mM DTT, 20 mM $MgCl_2$, 0.5 mM Na_3VO_4, 10 mM β-glycerophosphate, and 50 µM ATP). After aspirating the excess kinase buffer from the protein G beads, 40 µl kinase buffer, 3 µg myelin basic protein (M-1891; Sigma-Aldrich), and 5 µCi γ-[^{32}P]ATP (BLU502A; PerkinElmer) were immediately added and mixed with the DPak3-bound beads. The reactions were performed at 30°C for 30 min with the protein beads gently resuspended every 10 min. The proteins were eluted by 2x SDS running buffer and separated on a Bis-Tris Precast gel (Invitrogen). The phosphorylated bands were visualized by a typhoon imager and the amount of loaded proteins was determined by Coomassie brilliant blue staining.

For detecting the phosphorylation status of V5-DPak3 in *Drosophila* embryos, *V5-DPak3;dpak3*^{zyg}*/TM3,ftz-lacZ* females were crossed with *twi-GAL4;dpak3*^{zyg}*/TM3,ftz-lacZ* males. Stage 14 embryos were collected, homogenized, and subjected to SDS-PAGE and Western blot.

Confocal imaging of fixed samples

Images were obtained on a confocal microscope (LSM 700; Carl Zeiss) with a Plan-NeoFluar 40x/1.3 NA oil or Plan-Apochromat 63x/1.4 NA oil DIC objective, a pigtail-coupled solid-state laser with polarization-preserving single-mode fiber, and a high-sensitivity PMT detector. The pinhole was set to 1.0 AU for each channel and images were collected at 1.0-µm intervals. Images were acquired with Zen 2009 software (Carl Zeiss) and processed using Adobe Photoshop CS4. All samples were mounted in ProLong Gold Antifade reagent (Invitrogen) and imaged at room temperature.

Measurement of fluorescence intensity of F-actin foci

Fluorescence intensity was measured by using the overlay function of Zen 2009 and Photoshop CS4 extended software. Area of interest was defined by tracing the outline of the F-actin foci labeled by phalloidin as described previously (Sens et al., 2010). Specifically, to be included as part of the foci, the intensity of the phalloidin signal in the pixel had to be greater than the average intensity of the cortical actin. Foci were measured if they could be clearly assigned to one FCM and were distinct from other foci, to ensure that only a single focus was measured. Numbers shown in the text are relative intensities based on the 0–255 scale measured by the Zen 2009 software.

Time-lapse imaging

Embryos were collected, dechorionated with bleach, thoroughly washed, and gently attached onto a piece of clear acid-free double-sided tape (low auto-fluorescence, 6.3 mm; Therm O Web), which keeps embryos from rolling and drifting. Embryos were covered with a few drops of halocarbon oil to keep them moist while allowing adequate oxygen exchange. Subsequently, the embryos were covered with a 22 × 40–1.5 coverslip (Thermo Fisher Scientific) and the fluorescent GFP-actin was visualized with a Plan-NeoFluar 40x/1.3 NA oil objective. The solid-state laser output was set to 2% to avoid photobleaching and phototoxicity. Other confocal settings are

as follows: pinhole, 1 AU; z-stack, 1 µm step-wise, 4 µm total; and 4 frames averaged per scan. Zen 2009 and ImageJ 1.41h (National Institutes of Health, Bethesda, MD) were used to convert confocal images to movies.

Transmission electron microscopy

High-pressure freezing/freeze substitution (HPF/FS) fixation was performed as described previously (Zhang and Chen, 2008; Sens et al., 2010). In brief, a Bal-Tec device was used to freeze embryos. Freeze-substitution was performed using 1% osmium tetroxide and 0.1% uranyl acetate in 98% acetone and 2% methanol on dry ice. The embryos were embedded in Epon (Sigma-Aldrich). Thin sections (70 nm) were cut with a microtome (Ultracut R; Leica), mounted on copper grids, and post-stained with 5% uranyl acetate for 10 min and Sato's lead solution (1% $Pb(NO_3)_2$, 1% $C_{12}H_{10}O_{14}Pb_3$, 1% $(CH_3COO)_2Pb$, 2% $C_{12}H_{10}O_{14}Na_6$, and 0.72% NaOH) for 2 min to improve image contrast. Images were acquired on a transmission electron microscope (CM120; Philips).

Online supplemental material

Fig. S1 shows that muscle cell fate is properly specified in *dpak3* mutant embryos. Fig. S2 shows in situ hybridization of *dpak3* and *dpak1* in wild-type embryos. Fig. S3 shows specificity of the α-DPak1 and α-DPak3 antibodies. Video1 shows time-lapse imaging of an actin focus in a wild-type embryo expressing GFP-actin with the mesodermal driver *twi-GAL4*. Video 2 shows time-lapse imaging of an actin focus in a *dpak3* mutant embryo expressing GFP-actin with *twi-GAL4*. Table S1 shows mean numbers of nuclei in DA1 muscles of wild-type and fusion mutant embryos. Online supplemental material is available at http://www.jcb.org/cgi/content/full/jcb.201204065/DC1.

We thank Drs. S. Abmayr, H. Nguyen, N. Harden, D. Kiehart, D. Menon, B. Paterson, J. Zallen, and A. Zelhof for antibodies and fly stocks; Dr. R. Leapman at LBPH, NIH for access to the HPF/FS unit; and members of the Chen laboratory for helpful discussions and comments on the manuscript.

This work was supported by a grant from the National Institutes of Health to E.H. Chen (R01AR053173). P. Jin was a predoctoral fellow and R. Duan is a postdoctoral fellow of the American Heart Association.

Submitted: 12 April 2012
Accepted: 23 August 2012

References

Abmayr, S.M., and G.K. Pavlath. 2012. Myoblast fusion: lessons from flies and mice. *Development*. 139:641–656. http://dx.doi.org/10.1242/dev.068353

Abmayr, S.M., L. Balagopalan, B.J. Galletta, and S.J. Hong. 2003. Cell and molecular biology of myoblast fusion. *Int. Rev. Cytol.* 225:33–89. http://dx.doi.org/10.1016/S0074-7696(05)25002-7

Abo, A., J. Qu, M.S. Cammarano, C. Dan, A. Fritsch, V. Baud, B. Belisle, and A. Minden. 1998. PAK4, a novel effector for Cdc42Hs, is implicated in the reorganization of the actin cytoskeleton and in the formation of filopodia. *EMBO J.* 17:6527–6540. http://dx.doi.org/10.1093/emboj/17.22.6527

Adam, L., R. Vadlamudi, M. Mandal, J. Chernoff, and R. Kumar. 2000. Regulation of microfilament reorganization and invasiveness of breast cancer cells by kinase dead p21-activated kinase-1. *J. Biol. Chem.* 275:12041–12050. http://dx.doi.org/10.1074/jbc.275.16.12041

Albin, S.D., and G.W. Davis. 2004. Coordinating structural and functional synapse development: postsynaptic p21-activated kinase independently specifies glutamate receptor abundance and postsynaptic morphology. *J. Neurosci.* 24:6871–6879. http://dx.doi.org/10.1523/JNEUROSCI.1538-04.2004

Arias-Romero, L.E., and J. Chernoff. 2008. A tale of two Paks. *Biol. Cell*. 100:97–108. http://dx.doi.org/10.1042/BC20070109

Arias-Romero, L.E., O. Villamar-Cruz, A. Pacheco, R. Kosoff, M. Huang, S.K. Muthuswamy, and J. Chernoff. 2010. A Rac-Pak signaling pathway is essential for ErbB2-mediated transformation of human breast epithelial cancer cells. *Oncogene*. 29:5839–5849. http://dx.doi.org/10.1038/onc.2010.318

Artero, R.D., I. Castanon, and M.K. Baylies. 2001. The immunoglobulin-like protein Hibris functions as a dose-dependent regulator of myoblast fusion and is differentially controlled by Ras and Notch signaling. *Development*. 128:4251–4264.

Ayala, I., M. Baldassarre, G. Giacchetti, G. Caldieri, S. Tetè, A. Luini, and R. Buccione. 2008. Multiple regulatory inputs converge on cortactin to control invadopodia biogenesis and extracellular matrix degradation. *J. Cell Sci.* 121:369–378. http://dx.doi.org/10.1242/jcs.008037

Bahri, S.M., J.M. Choy, E. Manser, L. Lim, and X. Yang. 2009. The *Drosophila* homologue of Arf-GAP GIT1, dGIT, is required for proper muscle morphogenesis and guidance during embryogenesis. *Dev. Biol.* 325:15–23. http://dx.doi.org/10.1016/j.ydbio.2008.09.001

Bahri, S., S. Wang, R. Conder, J. Choy, S. Vlachos, K. Dong, C. Merino, S. Sigrist, C. Molnar, X. Yang, et al. 2010. The leading edge during dorsal closure as a model for epithelial plasticity: Pak is required for recruitment of the Scribble complex and septate junction formation. *Development*. 137:2023–2032. http://dx.doi.org/10.1242/dev.045088

Ben-Yaacov, S., R. Le Borgne, I. Abramson, F. Schweisguth, and E.D. Schejter. 2001. Wasp, the *Drosophila* Wiskott-Aldrich syndrome gene homologue, is required for cell fate decisions mediated by Notch signaling. *J. Cell Biol.* 152:1–13.

Benner, G.E., P.B. Dennis, and R.A. Masaracchia. 1995. Activation of an S6/H4 kinase (PAK 65) from human placenta by intramolecular and intermolecular autophosphorylation. *J. Biol. Chem.* 270:21121–21128. http://dx.doi.org/10.1074/jbc.270.36.21121

Bokoch, G.M. 2003. Biology of the p21-activated kinases. *Annu. Rev. Biochem.* 72:743–781. http://dx.doi.org/10.1146/annurev.biochem.72.121801.161742

Bour, B.A., M. Chakravarti, J.M. West, and S.M. Abmayr. 2000. *Drosophila* SNS, a member of the immunoglobulin superfamily that is essential for myoblast fusion. *Genes Dev.* 14:1498–1511.

Chen, E.H. 2011. Invasive podosomes and myoblast fusion. *Curr Top Membr*. 68:235–258. http://dx.doi.org/10.1016/B978-0-12-385891-7.00010-6

Chen, E.H., and E.N. Olson. 2004. Towards a molecular pathway for myoblast fusion in *Drosophila*. *Trends Cell Biol.* 14:452–460. http://dx.doi.org/10.1016/j.tcb.2004.07.008

Chong, C., L. Tan, L. Lim, and E. Manser. 2001. The mechanism of PAK activation. Autophosphorylation events in both regulatory and kinase domains control activity. *J. Biol. Chem.* 276:17347–17353. http://dx.doi.org/10.1074/jbc.M009316200

Claessens, M.M., M. Bathe, E. Frey, and A.R. Bausch. 2006. Actin-binding proteins sensitively mediate F-actin bundle stiffness. *Nat. Mater.* 5:748–753. http://dx.doi.org/10.1038/nmat1718

Conder, R., H. Yu, M. Ricos, H. Hing, W. Chia, L. Lim, and N. Harden. 2004. dPak is required for integrity of the leading edge cytoskeleton during *Drosophila* dorsal closure but does not signal through the JNK cascade. *Dev. Biol.* 276:378–390. http://dx.doi.org/10.1016/j.ydbio.2004.08.044

Conder, R., H. Yu, B. Zahedi, and N. Harden. 2007. The serine/threonine kinase dPak is required for polarized assembly of F-actin bundles and apical-basal polarity in the *Drosophila* follicular epithelium. *Dev. Biol.* 305:470–482. http://dx.doi.org/10.1016/j.ydbio.2007.02.034

Duan, H., J.B. Skeath, and H.T. Nguyen. 2001. *Drosophila* Lame duck, a novel member of the Gli superfamily, acts as a key regulator of myogenesis by controlling fusion-competent myoblast development. *Development*. 128:4489–4500.

Dworak, H.A., M.A. Charles, L.B. Pellerano, and H. Sink. 2001. Characterization of *Drosophila hibris*, a gene related to human nephrin. *Development*. 128:4265–4276.

Erickson, M.R., B.J. Galletta, and S.M. Abmayr. 1997. *Drosophila myoblast city* encodes a conserved protein that is essential for myoblast fusion, dorsal closure, and cytoskeletal organization. *J. Cell Biol.* 138:589–603. http://dx.doi.org/10.1083/jcb.138.3.589

Eswaran, J., M. Soundararajan, R. Kumar, and S. Knapp. 2008. UnPAKing the class differences among p21-activated kinases. *Trends Biochem. Sci.* 33:394–403. http://dx.doi.org/10.1016/j.tibs.2008.06.002

Galletta, B.J., M. Chakravarti, R. Banerjee, and S.M. Abmayr. 2004. SNS: adhesive properties, localization requirements and ectodomain dependence in S2 cells and embryonic myoblasts. *Mech. Dev.* 121:1455–1468. http://dx.doi.org/10.1016/j.mod.2004.08.001

Gatti, A., Z. Huang, P.T. Tuazon, and J.A. Traugh. 1999. Multisite autophosphorylation of p21-activated protein kinase gamma-PAK as a function of activation. *J. Biol. Chem.* 274:8022–8028. http://dx.doi.org/10.1074/jbc.274.12.8022

Geisbrecht, E.R., S. Haralalka, S.K. Swanson, L. Florens, M.P. Washburn, and S.M. Abmayr. 2008. *Drosophila* ELMO/CED-12 interacts with Myoblast city to direct myoblast fusion and ommatidial organization. *Dev. Biol.* 314:137–149. http://dx.doi.org/10.1016/j.ydbio.2007.11.022

Gildor, B., R. Massarwa, B.Z. Shilo, and E.D. Schejter. 2009. The SCAR and WASp nucleation-promoting factors act sequentially to mediate *Drosophila* myoblast fusion. *EMBO Rep.* 10:1043–1050. http://dx.doi.org/10.1038/embor.2009.129

Gringel, A., D. Walz, G. Rosenberger, A. Minden, K. Kutsche, P. Kopp, and S. Linder. 2006. PAK4 and alphaPIX determine podosome size and number in macrophages through localized actin regulation. *J. Cell. Physiol.* 209:568–579. http://dx.doi.org/10.1002/jcp.20777

Hakeda-Suzuki, S., J. Ng, J. Tzu, G. Dietzl, Y. Sun, M. Harms, T. Nardine, L. Luo, and B.J. Dickson. 2002. Rac function and regulation during *Drosophila* development. *Nature*. 416:438–442. http://dx.doi.org/10.1038/416438a

Haralalka, S., C. Shelton, H.N. Cartwright, E. Katzfey, E. Janzen, and S.M. Abmayr. 2011. Asymmetric Mbc, active Rac1 and F-actin foci in the fusion-competent myoblasts during myoblast fusion in *Drosophila*. *Development*. 138:1551–1562. http://dx.doi.org/10.1242/dev.057653

Harden, N., J. Lee, H.Y. Loh, Y.M. Ong, I. Tan, T. Leung, E. Manser, and L. Lim. 1996. A *Drosophila* homolog of the Rac- and Cdc42-activated serine/threonine kinase PAK is a potential focal adhesion and focal complex protein that colocalizes with dynamic actin structures. *Mol. Cell. Biol.* 16:1896–1908.

Hing, H., J. Xiao, N. Harden, L. Lim, and S.L. Zipursky. 1999. Pak functions downstream of Dock to regulate photoreceptor axon guidance in *Drosophila*. *Cell*. 97:853–863. http://dx.doi.org/10.1016/S0092-8674(00)80798-9

Hsu, R.M., M.H. Tsai, Y.J. Hsieh, P.C. Lyu, and J.S. Yu. 2010. Identification of MYO18A as a novel interacting partner of the PAK2/betaPIX/GIT1 complex and its potential function in modulating epithelial cell migration. *Mol. Biol. Cell*. 21:287–301. http://dx.doi.org/10.1091/mbc.E09-03-0232

Hummel, T., K. Leifker, and C. Klämbt. 2000. The *Drosophila* HEM-2/NAP1 homolog KETTE controls axonal pathfinding and cytoskeletal organization. *Genes Dev.* 14:863–873.

Jin, P., R. Duan, F. Luo, G. Zhang, S.N. Hong, and E.H. Chen. 2011. Competition between Blown fuse and WASP for WIP binding regulates the dynamics of WASP-dependent actin polymerization in vivo. *Dev. Cell*. 20:623–638. http://dx.doi.org/10.1016/j.devcel.2011.04.007

Kesper, D.A., C. Stute, D. Buttgereit, N. Kreisköther, S. Vishnu, K.F. Fischbach, and R. Renkawitz-Pohl. 2007. Myoblast fusion in *Drosophila melanogaster* is mediated through a fusion-restricted myogenic-adhesive structure (FuRMAS). *Dev. Dyn.* 236:404–415. http://dx.doi.org/10.1002/dvdy.21035

Kiehart, D.P., and R. Feghali. 1986. Cytoplasmic myosin from *Drosophila melanogaster*. *J. Cell Biol.* 103:1517–1525. http://dx.doi.org/10.1083/jcb.103.4.1517

Kim, S., K. Shilagardi, S. Zhang, S.N. Hong, K.L. Sens, J. Bo, G.A. Gonzalez, and E.H. Chen. 2007. A critical function for the actin cytoskeleton in targeted exocytosis of prefusion vesicles during myoblast fusion. *Dev. Cell*. 12:571–586. http://dx.doi.org/10.1016/j.devcel.2007.02.019

Kocherlakota, K.S., J.M. Wu, J. McDermott, and S.M. Abmayr. 2008. Analysis of the cell adhesion molecule sticks-and-stones reveals multiple redundant functional domains, protein-interaction motifs and phosphorylated tyrosines that direct myoblast fusion in *Drosophila melanogaster*. *Genetics*. 178:1371–1383. http://dx.doi.org/10.1534/genetics.107.083808

Lei, M., W. Lu, W. Meng, M.C. Parrini, M.J. Eck, B.J. Mayer, and S.C. Harrison. 2000. Structure of PAK1 in an autoinhibited conformation reveals a multistage activation switch. *Cell*. 102:387–397. http://dx.doi.org/10.1016/S0092-8674(00)00043-X

Massarwa, R., S. Carmon, B.Z. Shilo, and E.D. Schejter. 2007. WIP/WASp-based actin-polymerization machinery is essential for myoblast fusion in *Drosophila*. *Dev. Cell*. 12:557–569. http://dx.doi.org/10.1016/j.devcel.2007.01.016

Menon, S.D., and W. Chia. 2001. *Drosophila* rolling pebbles: a multidomain protein required for myoblast fusion that recruits D-Titin in response to the myoblast attractant Dumbfounded. *Dev. Cell*. 1:691–703. http://dx.doi.org/10.1016/S1534-5807(01)00075-2

Mentzel, B., and T. Raabe. 2005. Phylogenetic and structural analysis of the *Drosophila melanogaster* p21-activated kinase DmPAK3. *Gene*. 349:25–33. http://dx.doi.org/10.1016/j.gene.2004.12.030

Molli, P.R., D.Q. Li, B.W. Murray, S.K. Rayala, and R. Kumar. 2009. PAK signaling in oncogenesis. *Oncogene*. 28:2545–2555. http://dx.doi.org/10.1038/onc.2009.119

Morita, T., T. Mayanagi, T. Yoshio, and K. Sobue. 2007. Changes in the balance between caldesmon regulated by p21-activated kinases and the Arp2/3 complex govern podosome formation. *J. Biol. Chem.* 282:8454–8463. http://dx.doi.org/10.1074/jbc.M609983200

Morreale, A., M. Venkatesan, H.R. Mott, D. Owen, D. Nietlispach, P.N. Lowe, and E.D. Laue. 2000. Structure of Cdc42 bound to the GTPase binding domain of PAK. *Nat. Struct. Biol.* 7:384–388. http://dx.doi.org/10.1038/75158

Nguyen, H.T., R. Bodmer, S.M. Abmayr, J.C. McDermott, and N.A. Spoerel. 1994. D-mef2: a *Drosophila* mesoderm-specific MADS box-containing gene with a biphasic expression profile during embryogenesis. *Proc. Natl. Acad. Sci. USA*. 91:7520–7524. http://dx.doi.org/10.1073/pnas.91.16.7520

Ozdowski, E.F., S. Gayle, H. Bao, B. Zhang, and N.T. Sherwood. 2011. Loss of *Drosophila melanogaster* p21-activated kinase 3 suppresses defects in synapse structure and function caused by spastin mutations. *Genetics*. 189:123–135. http://dx.doi.org/10.1534/genetics.111.130831

Parks, A.L., K.R. Cook, M. Belvin, N.A. Dompe, R. Fawcett, K. Huppert, L.R. Tan, C.G. Winter, K.P. Bogart, J.E. Deal, et al. 2004. Systematic generation of high-resolution deletion coverage of the *Drosophila melanogaster* genome. *Nat. Genet.* 36:288–292. http://dx.doi.org/10.1038/ng1312

Parrini, M.C., M. Lei, S.C. Harrison, and B.J. Mayer. 2002. Pak1 kinase homodimers are autoinhibited in trans and dissociated upon activation by Cdc42 and Rac1. *Mol. Cell*. 9:73–83. http://dx.doi.org/10.1016/S1097-2765(01)00428-2

Paululat, A., A. Holz, and R. Renkawitz-Pohl. 1999. Essential genes for myoblast fusion in *Drosophila* embryogenesis. *Mech. Dev.* 83:17–26. http://dx.doi.org/10.1016/S0925-4773(99)00029-5

Pirruccello, M., H. Sondermann, J.G. Pelton, P. Pellicena, A. Hoelz, J. Chernoff, D.E. Wemmer, and J. Kuriyan. 2006. A dimeric kinase assembly underlying autophosphorylation in the p21 activated kinases. *J. Mol. Biol.* 361:312–326. http://dx.doi.org/10.1016/j.jmb.2006.06.017

Richardson, B.E., K. Beckett, S.J. Nowak, and M.K. Baylies. 2007. SCAR/WAVE and Arp2/3 are crucial for cytoskeletal remodeling at the site of myoblast fusion. *Development*. 134:4357–4367. http://dx.doi.org/10.1242/dev.010678

Rochlin, K., S. Yu, S. Roy, and M.K. Baylies. 2010. Myoblast fusion: when it takes more to make one. *Dev. Biol.* 341:66–83. http://dx.doi.org/10.1016/j.ydbio.2009.10.024

Ruiz-Gómez, M., N. Coutts, A. Price, M.V. Taylor, and M. Bate. 2000. *Drosophila* dumbfounded: a myoblast attractant essential for fusion. *Cell*. 102:189–198. http://dx.doi.org/10.1016/S0092-8674(00)00024-6

Rushton, E., R. Drysdale, S.M. Abmayr, A.M. Michelson, and M. Bate. 1995. Mutations in a novel gene, myoblast city, provide evidence in support of the founder cell hypothesis for *Drosophila* muscle development. *Development*. 121:1979–1988.

Schäfer, G., S. Weber, A. Holz, S. Bogdan, S. Schumacher, A. Müller, R. Renkawitz-Pohl, and S.F. Onel. 2007. The Wiskott-Aldrich syndrome protein (WASP) is essential for myoblast fusion in *Drosophila*. *Dev. Biol.* 304:664–674. http://dx.doi.org/10.1016/j.ydbio.2007.01.015

Schneeberger, D., and T. Raabe. 2003. Mbt, a *Drosophila* PAK protein, combines with Cdc42 to regulate photoreceptor cell morphogenesis. *Development*. 130:427–437. http://dx.doi.org/10.1242/dev.00248

Schröter, R.H., S. Lier, A. Holz, S. Bogdan, C. Klämbt, L. Beck, and R. Renkawitz-Pohl. 2004. *kette* and *blown fuse* interact genetically during the second fusion step of myogenesis in *Drosophila*. *Development*. 131:4501–4509. http://dx.doi.org/10.1242/dev.01309

Sens, K.L., S. Zhang, P. Jin, R. Duan, G. Zhang, F. Luo, L. Parachini, and E.H. Chen. 2010. An invasive podosome-like structure promotes fusion pore formation during myoblast fusion. *J. Cell Biol.* 191:1013–1027. http://dx.doi.org/10.1083/jcb.201006006

Shelton, C., K.S. Kocherlakota, S. Zhuang, and S.M. Abmayr. 2009. The immunoglobulin superfamily member Hbs functions redundantly with Sns in interactions between founder and fusion-competent myoblasts. *Development*. 136:1159–1168. http://dx.doi.org/10.1242/dev.026302

Stofega, M.R., L.C. Sanders, E.M. Gardiner, and G.M. Bokoch. 2004. Constitutive p21-activated kinase (PAK) activation in breast cancer cells as a result of mislocalization of PAK to focal adhesions. *Mol. Biol. Cell*. 15:2965–2977. http://dx.doi.org/10.1091/mbc.E03-08-0604

Strünkelnberg, M., B. Bonengel, L.M. Moda, A. Hertenstein, H.G. de Couet, R.G. Ramos, and K.F. Fischbach. 2001. *rst* and its paralogue *kirre* act redundantly during embryonic muscle development in *Drosophila*. *Development*. 128:4229–4239.

Tang, Y., Z. Chen, D. Ambrose, J. Liu, J.B. Gibbs, J. Chernoff, and J. Field. 1997. Kinase-deficient Pak1 mutants inhibit Ras transformation of Rat-1 fibroblasts. *Mol. Cell. Biol.* 17:4454–4464.

Thompson, G., D. Owen, P.A. Chalk, and P.N. Lowe. 1998. Delineation of the Cdc42/Rac-binding domain of p21-activated kinase. *Biochemistry*. 37:7885–7891. http://dx.doi.org/10.1021/bi980140+

Vadlamudi, R.K., and R. Kumar. 2003. P21-activated kinases in human cancer. *Cancer Metastasis Rev.* 22:385–393. http://dx.doi.org/10.1023/A:1023729130497

Vadlamudi, R.K., L. Adam, R.A. Wang, M. Mandal, D. Nguyen, A. Sahin, J. Chernoff, M.C. Hung, and R. Kumar. 2000. Regulatable expression of p21-activated kinase-1 promotes anchorage-independent growth and abnormal organization of mitotic spindles in human epithelial breast cancer cells. *J. Biol. Chem.* 275:36238–36244. http://dx.doi.org/10.1074/jbc.M002138200

Weaver, A.M. 2006. Invadopodia: specialized cell structures for cancer invasion. *Clin. Exp. Metastasis*. 23:97–105. http://dx.doi.org/10.1007/s10585-006-9014-1

Webb, B.A., R. Eves, S.W. Crawley, S. Zhou, G.P. Côté, and A.S. Mak. 2005. PAK1 induces podosome formation in A7r5 vascular smooth muscle cells in a PAK-interacting exchange factor-dependent manner. *Am. J. Physiol. Cell Physiol.* 289:C898–C907. http://dx.doi.org/10.1152/ajpcell.00095.2005

Whale, A., F.N. Hashim, S. Fram, G.E. Jones, and C.M. Wells. 2011. Signalling to cancer cell invasion through PAK family kinases. *Front. Biosci.* 16:849–864. http://dx.doi.org/10.2741/3724

Zallen, J.A., Y. Cohen, A.M. Hudson, L. Cooley, E. Wieschaus, and E.D. Schejter. 2002. SCAR is a primary regulator of Arp2/3-dependent morphological events in *Drosophila*. *J. Cell Biol.* 156:689–701. http://dx.doi.org/10.1083/jcb.200109057

Zhang, S., and E.H. Chen. 2008. Ultrastructural analysis of myoblast fusion in *Drosophila*. *In* Cell Fusion: Overviews and Methods. E.H. Chen, editor. Humana Press, NJ. 275–297.

Zhao, Z.S., E. Manser, X.Q. Chen, C. Chong, T. Leung, and L. Lim. 1998. A conserved negative regulatory region in alphaPAK: inhibition of PAK kinases reveals their morphological roles downstream of Cdc42 and Rac1. *Mol. Cell. Biol.* 18:2153–2163.